Phevamine A, a bacterial small molecule that suppresses plant immune response

Supporting Information Appendix

Erinn M. O'Neill, Tatiana S. Mucyn, Jon B. Patteson, Omri M. Finkel, Eui-Hwan Chung, Joshua A. Baccile, Elisabetta Massolo, Frank C. Schroeder, Jeffery L. Dangl, and Bo Li

Materials and Methods

General

All chemicals were purchased from Sigma-Aldrich or Fisher. Primers were ordered from Integrated DNA Technology (Table S3). Polymerase, restriction enzymes, and ligase were purchased from New England Biolabs. DNA manipulation kits were purchased from Qiagen and Thermo Scientific. PCR reactions were carried out using an Eppendorf Nexus GSX1 thermocycler with Q5 DNA polymerase. General genetic manipulation of *E. coli* was carried out using standard protocols (1). LC-MS data was obtained using an Agilent 6520 accurate-mass Q-TOF LC/MS. Preparative HPLC was carried out using a Phenomenex Luna 10 µm C18 (2) column on a Varian Prostar instrument equipped with a PDA detector. Further purification was carried out using a Phenomenex Kinetex 5 µm C18 column (100 Å, 150 mm x 4.60 mm) on a Shimadzu HPLC equipped with an SPD-20A UV-vis detector. NMR spectra were obtained using a Bruker 600 MHz spectrometer or a Bruker Avance^{III} HD 800 MHz spectrometer unless otherwise noted.

Bacterial strains and culture conditions

For cloning, *E. coli* DH5α and *E. coli* Top10 chemically competent maximum efficiency cells were used (Invitrogen). For heterologous expression, *E. coli* BL21(DE3) chemically competent cells (Agilent) were transformed with vectors containing *hsv* expression constructs (Table S4). The *hrpL* expression construct in pBAD vector was previously described (2). All overnight seed cultures were inoculated with a single colony and grown in 5 mL media in 14 mL Falcon culture tubes. Antibiotics were used in these concentrations, unless otherwise noted: 10 µg/mL tetracycline, 25 µg/mL chloramphenicol, 50 µg/mL kanamycin, 50 µg/mL spectinomycin, or 100 µg/mL ampicillin. All cultures for metabolomics were grown in 100 mL media with the appropriate antibiotic and 100 µL−2 mL of a saturated overnight culture. All *E. coli* cultures were grown in LB Media (Miller, granulated, Fisher) at 37 °C to an OD_{600} between 0.4 and 0.8. *E. coli* cultures were induced with 0.5 mM IPTG and then were incubated at 16 °C overnight, shaking at 225 rpm. *P. syringae* and *P. fluorescens* starter cultures were grown overnight in King's B Media (20 g/L Bacto Proteose Peptone #3, 1% glycerol by volume, 1.5 g/L K_2HPO_4, and 0.734 g/L $MgSO_4$, dissolved in water). *P.*

syringae cultures containing the pBAD plasmid were induced with 0.2% L-arabinose. All other *P. syringae* pv. *tomato* DC3000 and *P. fluorescens* cultures were not induced. Wildtype *P. fluorescens Pf*0-1 harboring the *hsv*-pBBR5 vector was grown in the presence of 50 µg/mL ampicillin and 50 µg/mL gentamycin. *P. fluorescens* harboring both *hsv*-pBBR5 and the T3SS (*Pf*0-1 +T3SS) was grown with 25 µg/mL tetracycline and 50 µg/mL gentamycin. After reaching an OD_{600} of >0.6 in King's B media, *P. fluorescens* and *P. syringae* cultures were washed with 100 mM $MgCl_2$ and resuspended in minimal media (12.8 g/L Na_2HPO_4 ● 7 H_2O, 3 g/L KH_2PO_4, 0.5 g/L NaCl, 1 g/L NH_4Cl, 1% glycerol by volume, 0.024 g/L $MgSO_4$, 0.0011 g/L $CaCl_2$, and 0.18 g/L mannitol, dissolved in water). Once resuspended in minimal media, these cultures were grown at 28 °C overnight and 16 °C for another 24 hours shaking at 225 rpm.

Protein expression and purification

Large-scale cultures for protein purification were grown in 1 L of media containing the appropriate antibiotic and 1−5 mL of overnight culture. At an OD600 of 0.5−0.8, a sample of 0.5 mM IPTG was added to induce protein expression. After 16 hours of protein expression, cultures were spun down and resuspended in HEPES lysis buffer (50 mM HEPES, 150 mM NaCl, 10% glycerol, pH 7.5). Cells were lysed by sonication at 30% amplitude for 3 minutes (0.5 seconds on and 1.5 seconds off). Cell debris was removed by centrifugation at 17,000 rpm for 40 minutes and the supernatant was filtered using a 0.45 µm filter (Corning). Each Hsv protein was purified using an AKTA FPLC using a 5 mL HiTrap nickel column (GE) at a flow rate of 3.0 mL/min. Wash buffer consisted of 50 mM HEPES, 150 mM NaCl, 25 mM imidazole, and 10% glycerol (pH 7.5). Elution buffer was the wash buffer with the addition of 250 mM imidazole. The wash step lasted for 5 column volumes (CVs). The proteins were eluted using a gradient of 0−100% of elution buffer over 10 CVs, and then held at 100% for 5 CVs. HsvB and HsvC were further purified using a HiLoad 16/600 Superdex 200 prep grade size exclusion column (GE) on the FPLC using the lysis buffer described above. The column was equilibrated with lysis buffer at a flow rate of 0.5 mL/min for 1.5 CVs, then

protein was loaded onto the column and eluted over 1.5 CVs using the same buffer and flow rate.

Amidinotransferase substrate assay conditions

To identify the preferred substrates of the amidinotransferase protein HsvA, L-arginine was incubated with potential substrates that accept the amidino group. Each reaction mixture contained two amino acids at 10 mM each (L-Arg and L-Lys, L-Arg and spermidine, or L-Arg and spermine). Each mixture also contained 100 mM HEPES (pH 7.5) and 20 µM purified HsvA to a final volume of 50 µL. Samples were incubated at 37 °C for 2 hours. Enzymes were omitted in negative controls. A sample of 10 µL was injected onto a Gemini C18 column (Phenomenex) on LC-MS and separated with a gradient of 2−73% acetonitrile (0.1% formic acid) over 25 minutes. This assay showed that HsvA catalyzes the transfer of the amidino group from L-Arg to spermidine, spermine, or L-lysine. Based on peak areas, the amidinospermidine product is present at the highest level, suggesting spermidine is the preferred substrate.

ATP-grasp substrate assay conditions

A malachite green dye assay (P_iColorLock, Innova Biosciences) was used to identify the preferred substrates of the ATP-grasp enzyme HsvB by quantifying free phosphate (P_i) release. Substrate assays were conducted in 100 µL scale in a microcentrifuge tube, and consisted of 2.0 mM amino acids, 10 µM of each enzyme, 10 mM $MgCl_2$, 5 mM ATP, and 50 mM HEPES (pH 7.5). After 30 minutes, reactions were diluted 1 in 10 with DI water into a 96-well plate to a final volume of 200 µL, then 50 µL Gold mix reagent and 20 µL stabilizer were added. After 30 minutes of incubation, UV-vis absorption of the products at 635 nm was measured on a Tecan infinite M1000 Pro plate reader. Assays containing L-Phe produced the most P_i, indicating that HsvB preferentially activates L-Phe.

Characterization of phevamine biosynthetic pathway

Sequential assays were conducted to elucidate the biosynthesis of phevamine A. Based on the structures of prephevamine, amidinotransfer by HsvA or condensation with L-Val

by HsvC may occur as the first step. This rationale led us to examine three potential biosynthetic pathways: HsvA → C → B, HsvC → A → B, and HsvC → B → A. An initial assay was conducted for either HsvA or HsvC. The HsvA assay consisted of 10 mM L-arginine, 10 mM spermidine, 100 mM HEPES (pH 7.5), 20 µM HsvA, and water in a 100 µL volume. Protein was removed after a 30 minute incubation at room temperature using a 3000 Da Amicon Ultra filter (Millipore) and the small molecule filtrate was collected. To this assay mixture, we added 2 mM $MgCl_2$, 1 mM ATP, 2 mM L-valine, and 10 µM HsvC. Protein was again removed after 30 minutes at room temperature with a 3000 Da filter and an aliquot was collected for LC-MS analysis. Finally, 2 mM L-phenylalanine and 10 µM HsvB were added, and the reaction was incubated at room temperature for 30 minutes before the reaction was quenched with acetonitrile at a ratio of 1:1 for 15 minutes, precipitated protein was removed by centrifugation, and the supernatant was analyzed by LC-MS. The initial HsvC assays consisted of 2 mM spermidine, 2 mM L-valine, 100 mM HEPES (pH 7.5), 2 mM $MgCl_2$, 1 mM ATP, 10 µM HsvC, and water in a 100 µL volume. After 30 minutes at room temperature, HsvC was removed with a 3000 Da filter. To one set of assays, 10 mM L-arginine and 20 µM HsvA were added. To the other set of assays, 2 mM L-phenylalanine and 10 µM HsvB were added. Both sets of reactions were incubated at room temperature for 30 minutes before removing protein with a 3000 Da filter. Aliquots were taken for LC-MS analysis. These reactions were then incubated with the remaining constituents that had not been added: 2 mM L-phenylalanine and 10 µM HsvB or 10 mM L-arginine and 20 µM HsvA. Reactions were incubated at room temperature for 30 minutes before they were quenched with acetonitrile at a ratio of 1:1 and the precipitated protein was removed by centrifugation. All aliquots were diluted 5 folds with water for LC-MS analysis. Phevamines were only produced when the reaction order was HsvA → HsvC → HsvB (Figure S10).

Purification of phevamine A

Assay supernatants were concentrated under reduced pressure and injected onto the prep HPLC at a flow rate of 15 mL/min with water and acetonitrile (both containing 0.1% trifluoroacetic acid) as mobile phases. The solvent gradient was held at 2% acetonitrile

for 10 minutes, then 5% acetonitrile for 5 minutes, and 10% acetonitrile for 15 minutes, before being ramped up to 95% over another 20 minutes. Fractions containing phevamine A (28–30 min retention time) were concentrated under reduced pressure and injected onto the analytical HPLC using the same mobile phases as those for the prep HPLC. The solvent gradient ramped from 2−30% acetonitrile over 35 minutes before ramping up to 95% for another 8 minutes (flow rate: 0.5 mL/min). Fractions containing phevamine A were collected at retention times of 20−25 minutes, and concentrated. To separate the two regio-isomers, a final round of purification was conducted on the analytical HPLC with an extended gradient at 10−20% acetonitrile for 25 min. Specifically, the solvent gradient started at 2−5% acetonitrile over 5 minutes, then 5−10% over another 5 minutes, and finished with 10−20% for another 25 minutes (flow rate: 0.5 mL/min). Fractions with retention times between 17.5–19.5 minutes were collected and concentrated. LC/MS analysis showed that the concentrated sample contained ~95% pure phevamine A (67% yield).

NMR spectroscopy for phevamine A and B

All spectra for *in vitro* purified phevamine A and B were obtained using a Bruker Avance^{III} HD (800 MHz ^{1}H reference frequency, 201 MHz for ^{13}C) equipped with a 5 mm CPTCL ^{1}H-^{13}C/^{15}N cryo probe. Non-gradient phase-cycled dqfCOSY spectra were acquired using the following parameters: 0.6 s acquisition time, 400−600 complex increments, 8, 16 or 32 scans per increment. Non-gradient HSQC and HMBC spectra were acquired with these parameters: 0.25 s acquisition time, 200−500 complex increments, 8−64 scans per increment. ^{1}H, ^{13}C-HMBC spectra were optimized for $J_{H,C}$ = 6 Hz. HSQC spectra were acquired without decoupling. NMR spectra were processed and baseline corrected using Mestrelabs MNOVA software packages. NMR assignments are shown in Tables S5 and S6.

Metabolite dependence on T3SS

The *hsv* operon was cloned into the pBBR5 plasmid containing a constitutive promoter and gentamycin resistance marker (3). *P. fluorescens Pf*0-1 and *Pf*0-1 + T3SS were both transformed with *hsv*-pBBR5 by electroporation using the method described by

Choi and Schweizer (4). Cultures (100 mL) were grown and extracted as described above to detect phevamine production and determine whether phevamine secretion is dependent on T3SS (Fig. S7).

Generation of Pseudomonas clean deletion mutants

Pseudomonas knockout clones were generated using MTN1907, a modified version of pLVC-D, which allows for *SacB* counter-selection (2, 5, 6). Overlapping primers MT1881, MT1880, MT1877, and MT1878 (Table S3) were used to generate a chimeric fragment composed of the ~200 bp sequence upstream of *hsvA* fused to the ~200bp region downstream of *hsvC*. The chimeric fragment was sub-cloned into MTN1907 and *Pseudomonas* was transformed with the plasmid to obtain a merodiploid after recombination. Two merodiploids, with a 3' end and a 5' end insertion, were selected to generate two independent *Pseudomonas* clones with clean *hsv* deletion for each parental strain (*Pto* DC3000, *Pto*-Cor $^{-}$, *Pto*Δ*hrcC*, *Pto*D28E) after growth on media containing 5% sucrose for the second recombination (see Fig. S29 and S30). For complementation, the *hsv* operon was sub-cloned into pBAV226 downstream of the *NptII* promoter (8) and transformed into *Pto*D28EΔ*hsv2* (see Fig. S30). The pBAV226 vector contains the sequence encoding the HA-tag downstream of the gateway cassette, but the HA tag was not included in the product of *hsvC* because the stop codon was retained.

Calcium burst measurement

Leaf disks of 3- to 4-week-old *A. thaliana* lines pMAQ2 expressing the apoaequorin gene under the control of the cauliflower mosaic virus 35S promoter (7) were collected in a 96-well plate and incubated overnight with 100 µM coelenterazine native (BYOSYNTH) (7). Luminescence was measured as in the ROS burst assay, with the exception that luminol and HRP were excluded from the reaction mix.

Synthesis of phevamine A

General information

Chemicals were purchased from commercial suppliers and used without further purification. Fmoc-derivatized amino acids were purchased from Alfa Aesar. N^1, N^4-bis-boc-spermidine was purchased from Chem-Impex International. Diethylamine and DIPEA were purchased from Sigma-Aldrich. *N,N′*-Di-Boc-1H-pyrazole-1-carboxamidine and trifluoroacetic acid were purchased from Acros Organics. HATU was purchased from Oakwood Products Inc. NMR solvents were purchased from Cambridge Isotope Laboratories. Normal-phase column chromatography was performed on silica gel (230−400 mesh). Reversed-phase chromatography was performed on C18-bonded silica, either on Phenomenex Kinetex C18 or Phenomenex Luna C18. High-resolution mass spectra (HRMS) were obtained using an Agilent 6520 Q-TOF LC/MS. Proton, carbon and fluorine magnetic resonance spectra (^{1}H NMR, ^{13}C NMR, and ^{19}F NMR) were recorded on a Bruker model DRX 400 or 600 (^{1}H NMR at 400 MHz or 600 MHz, ^{13}C NMR at 101 MHz or 151 MHz) or on a Bruker AVANCE III-OneBay500 (^{13}C NMR at 235 MHz) spectrometer. NMR experiments are reported in δ units, parts per million (ppm), and were referenced to $CDCl_3$ (δ 7.26 ppm for ^{1}H and 77.0 ppm for ^{13}C), DMSO (2.50 ppm), MeOD (3.31 ppm) or D_2O (4.79 ppm) as internal standards. ^{1}H NMR data are reported as follows: chemical shift, multiplicity (s = singlet, bs = broad singlet, d = doublet, dd = doublet of doublets, t = triplet, td = triplet of doublets, m = multiplet), coupling constants (Hz), and integration.

_N_-Boc-1,3-diaminopropane (1)

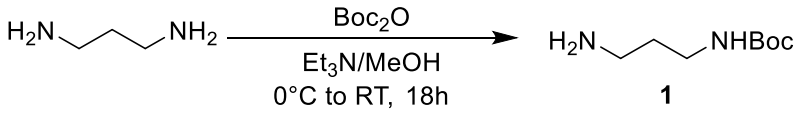

1

This synthesis followed a similar procedure as Kaur *et al.* (8). 1,3-Diaminopropane (3 g, 40.5 mmol, 1 eq.) was dissolved in a 10% solution of Et_3N in MeOH (30 mL); the mixture was cooled to 0 °C. In a flame dried flask, di-*tert*-butyl dicarbonate (4.4 g, 20 mmol, 0.5 eq.) was dissolved in MeOH and added to the cooled solution (via addition funnel). The reaction mixture, which did not appear homogeneous, was stirred overnight at room temperature (RT). The solvent was then removed under reduced pressure. The

crude mixture was treated with 10% Na_2CO_3 (10 mL, three times) and extracted with CH_2Cl_2. The combined organic phases were dried over anhydrous Na_2SO_4 and the solvent was removed under reduced pressure. The desired product (**1**) was obtained as a white solid (1.65 g, 23% yield) and used in the subsequent step without further purification.

^{1}H NMR (400 MHz, $CDCl_3$) δ 1.20 (bs, 1H), 1.44 (s, 9H), 1.64-1.57 (m, 2H), 2.76 (t, J = 6.6 Hz, 2H), 3.22-3.16 (m, 2H), 4.90 (bs, 1H).

N-(4-(3-Boc-1,3-diaminopropane)butyl)phthalimide (2)

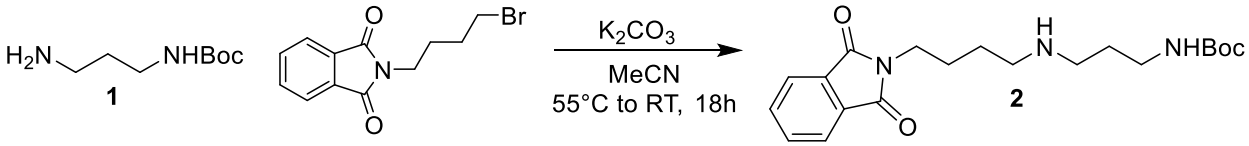

This reaction followed a procedure similar to that used by Wang *et al.* (2012) (9). *N*-Boc-1,3-diaminopropane (1.38 g, 7.9 mmol, 1.1 eq.) was dissolved in MeCN (15 mL) at RT and K_2CO_3 (3.43 g, 24.8 mmol, 5 eq.) was added. *N*-(4-Bromobutyl)phthalimide (2.2 g, 7.7 mmol, 1 eq.) was then added and the reaction mixture was heated to 50 °C and stirred at this temperature for 18 hours. Subsequently, the mixture was warmed up to RT and treated with H_2O. The mixture was extracted with EtOAc; the combined organic phases were dried over anhydrous Na_2SO_4 and the solvent was removed under reduced pressure. The desired product (**2**) was obtained (3 g, quantitative yield) and used in the subsequent step without further purification.

^{1}H NMR (400 MHz, $CDCl_3$) δ 1.90−1.82 (m, 2H), 1.40 (bs, 9H), 1.65-1.56 (m, 2H), 1.75−1.69 (m, 2H), 2.39−2.36 (m, 2H), 3.20-3.13 (m, 4H), 3.71−3.64 (m, 2H), 4.96 (bs, 1H), 7.75−7.72 (m, 2H), 7.82−7.79 (m, 2H),

N-(4-(*N*^{1},*N*^{3}-bis-Boc-1,3-diaminopropane)butyl)phthalimide (3)

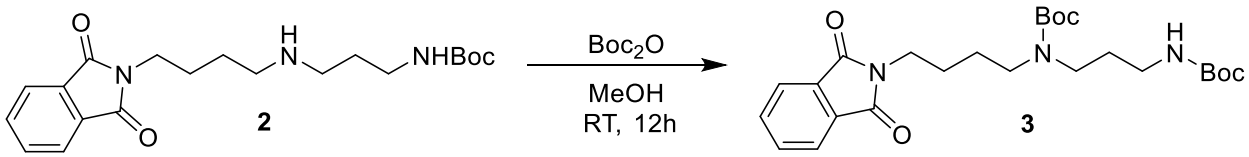

This reaction followed a similar procedure to that was used by Wang *et al.* (2014) (10). The substrate was dissolved in methanol (40 mL) and di-*tert*-butyl dicarbonate (1.7 g,

7.8 mmol, 1 eq.) was added. The reaction mixture was stirred at RT for 12 hours, then the solvent was removed under reduced pressure. The Boc-bisprotected product (**3**) was obtained as a pale, yellow oil (3.3 g, 87% yield) and used in the subsequent step without further purification.

^{1}H NMR (400 MHz, $CDCl_3$) δ 1.45−1.44 (m, 2H), 1.70−1.67 (m, 5H), 1.95−1.85 (m, 1H), 2.42 (bs, 2H), 3.27−3.10 (m, 4H), 3.76−3.70 (m, 2H), 7.75−7.72 (m, 2H), 7.88−7.84 (m, 2H).

***N*^{1}, *N*^{4}-bis-Boc-spermidine (4)**

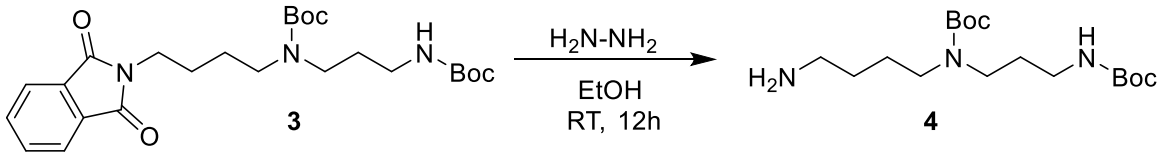

This reaction used a procedure similar to that was used by Wang *et al.* (2014) (10). To a solution of *tert*-butyl (3-((tert-butoxycarbonyl)amino)propyl)(4-(1,3-dioxoisoindolin-2-yl)butyl)carbamate (**3**) (780 mg, 1.64 mmol) in EtOH (30 mL), hydrazine hydrate (0.83 mL) was added and the reaction mixture was stirred for 12 hours at RT. The solvent was removed under reduced pressure and the residue was suspended in 10% ammonia and extracted with $CHCl_3$; the combined organic phases were dried on anhydrous Na_2SO_4 and the solvent was removed under reduced pressure. The desired product (**4**) was obtained as a pale, yellow oil (340 mg, 60% yield) and used in the subsequent step without further purification.

^{1}H NMR (400 MHz, $CDCl_3$) δ 1.48−1.46 (m. 18H), 1.66−1.57 (m, 7H), 2.43−2.40 (m, 1H), 2.49−2.46 (m, 1H), 2.74−2.71 (m, 1H), 3.26−3.12 (m, 4H), 3.69 (bs, 1H), 4.90 (bs, 1H), 5.78, 5.64 (bs 1H).

Fmoc-(*S*)-Val-bis-Boc-spermidine (5)

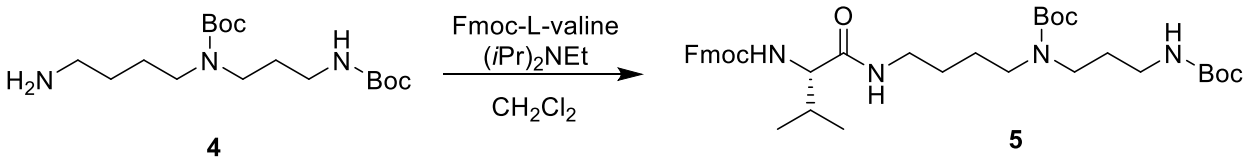

To a solution of N^1, N^4-bis-Boc-spermidine (**4**) (250 mg, 0.724 mmol, 1.0 eq.) in CH_2Cl_2 (20 mL) on ice, Fmoc-Val-OH (295 mg, 8.68 mmol, 1.2 eq.), and DIPEA (252.2 µL, 1.448 mmol, 2.0 eq.) were added. The reaction was stirred at room temperature for 16 hours. The crude reaction mixture was purified by flash chromatography (hexanes/ethyl acetate gradient) to afford pure product (**5**) (310 mg, 64% yield) as a white solid.

^{1}H NMR (400 MHz, $CDCl_3$) δ 0.97 (m, 6H), 1.46 (s, 9H), 1.47 (s, 9H), 1.52 (m, 2H), 1.66 (m, 2H), 2.15 (m, 2H), 3.07-3.35 (m, 9H), 4.23 (t, J = 7.0 Hz, 1H), 4.36 (m, 1H) 4.44 (m, 1H), 7.32 (t, J = 7.4 Hz, 2H), 7.42 (t, J = 7.6 Hz, 2H), 7.61 (d, J= 7.6 Hz, 2H), 7.78 (d, J = 7.2 Hz, 2H).

Fmoc-(*S*)-Phe-(*S*)-Val-bis-Boc-spermidine (6)

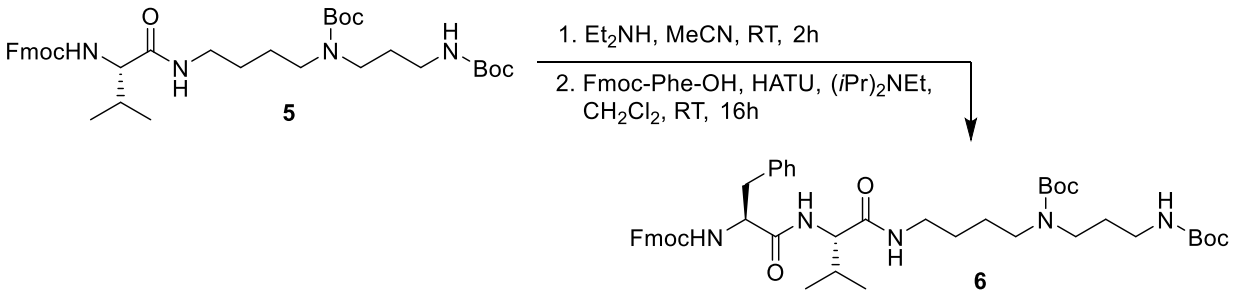

To a solution of Fmoc-(S)-Val-bis-Boc-spermidine (**5**) (310 mg, 0.465 mmol, 1.0 eq) in 20 mL MeCN, diethylamine (500 µL, 2.5% v/v) was added. The reaction was stirred at room temperature for 2 hours. The crude reaction mixture was concentrated under reduced pressure. Ethyl acetate (25 mL) was added, and the reaction mixture was concentrated again. The crude reaction mixture was dissolved in CH_2Cl_2 (20 mL) and added to a mixture of Fmoc-Phe-OH (216 mg, 0.558 mmol, 1.2 eq.), HATU (269 mg, 0.6975 mmol, 1.5 eq.), and DIPEA (162 µL, 0.742 mmol, 2.0 eq.) previously kept under stirring for 20 minutes on ice. The reaction was stirred at room temperature for 16 hours. The crude reaction mixture was purified by flash chromatography (hexanes/ethyl acetate gradient) to afford pure product (**6**) (190 mg, 50% yield) as a white solid.

^{1}H NMR (400 MHz, $CDCl_3$) δ 0.87 (d, J = 6.8 Hz, 3H), 0.92 (d, J = 6.8 Hz, 3H), 1.47 (s, 18H), 1.51 (m, 2H), 1.69 (m, 2H), 2.19 (m, 2H), 3.05−3.35 (m, 11H), 4.19 (t, 1H), 4.31 (m, 1H), 4.41 (m, 1H), 4.51 (m, 1H), 7.20 (m, 2H), 7.31 (m, 5H), 7.41 (t, J = 7.4 Hz, 2H), 7.54 (d, J = 7.6 Hz, 2H), 7.77 (d, J = 7.2 Hz, 2H).

Fmoc-(*S*)-Phe-(*S*)-Val-spermidine (7)

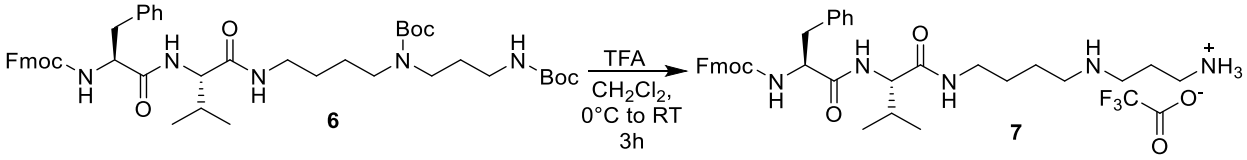

A solution of Fmoc-(*S*)-Phe-(*S*)-Val-bis-Boc-spermidine (**6**) (60 mg, 0.072 mmol) in CH_2Cl_2 (2 mL) was cooled to 0 °C and 800 µL of trifluoroacetic acid was added dropwise. The reaction was stirred at room temperature for 3 hours. The crude reaction mixture was concentrated under reduced pressure. Toluene was added, and the sample was concentrated under reduced pressure until dry. The pure product (**7**) (23 mg, 32% yield over two steps) was obtained as a white solid: ^{1}H NMR (400 MHz, MeOD) *δ* 0.96 (m, 6H), 1.59 (m, 2H), 1.70 (m, 2H), 2.07 (m, 3H), 3.00−3.27 (m, 10H), 4.08 (d, *J* = 7.2 Hz, 1H), 4.16 (t, *J* = 7.0 Hz, 1H), 4.26 (m, 1H), 4.34 (m, 1H), 4.42 (m, 1H), 7.16 (m, 1H), 7.21−7.32 (m, 5H), 7.40 (t, *J* = 7.6 Hz, 2H), 7.58 (d, *J* = 7.6 Hz, 2H), 7.81 (d, *J* = 7.6 Hz, 2H); HRMS (EI) *m/z* $[M + H]^+$ Calculated for $C_{36}H_{48}N_5O_4$ 614.370, observed 614.371.

Fmoc-(*S*)-Phe-(*S*)-Val-spermidine-*N,N'*-di-Boc-1*H*-guanidine (8)

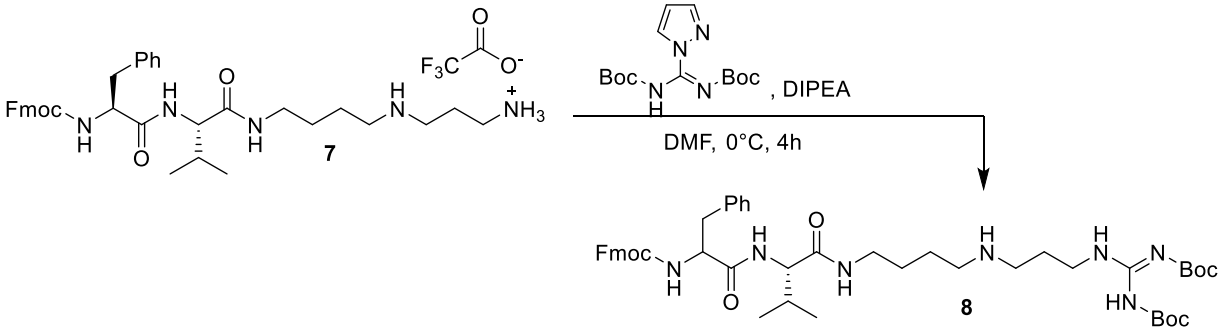

To a solution of Fmoc-(S)-Phe-(S)-Val-spermidine (**7**) in DMF (2 mL), which has been cooled to 0 °C, DIPEA (200 µL) and *N,N'*-Di-Boc-1H-pyrazole-1-carboxamidine (24 mg, 0.072 mmol, 1.0 eq.) were added. The reaction was stirred for 4 hours at room temperature. The crude reaction mixture was purified directly using reverse-phase prep HPLC (Phenomenex Luna C18, H_2O/MeCN gradient) and then purified using a second round of reverse-phase HPLC (Phenomenex Kinetex C18, H_2O/MeCN gradient). The product (**8**) was purified as a white solid (23 mg, 37% yield over 2 steps). ^{1}H NMR (600 MHz, MeOD) *δ* 0.96 (m, 6H), 1.49 (s, 9H), 1.55 (s, 9H), 1.60 (m, 2H), 1.72 (m, 2H), 1.95 (m, 2H), 2.07 (m, 1H), 3.02 (m, 4H), 3.14−3.23 (m, 2H), 3.24-3.35 (m, 2H) 3.47 (m, 2H),

4.08 (d, *J* = 7.2 Hz, 1H), 4.17 (t, *J* = 7.5 Hz, 1H), 4.26 (m, 1H), 4.35 (m, 1H), 4.42 (m, 2H), 7.23 (m, 2H), 7.30 (m, 5H), 7.40 (m, 2H), 7.58 (t, *J* = 6.9 Hz, 2H), 7.81 (d, *J* = 7.8 Hz, 2H); HRMS (EI) *m/z* $[M + H]^+$ Calculated for $C_{47}H_{66}N_7O_8$ 856.497, observed 856.499.

Phevamine A (9)

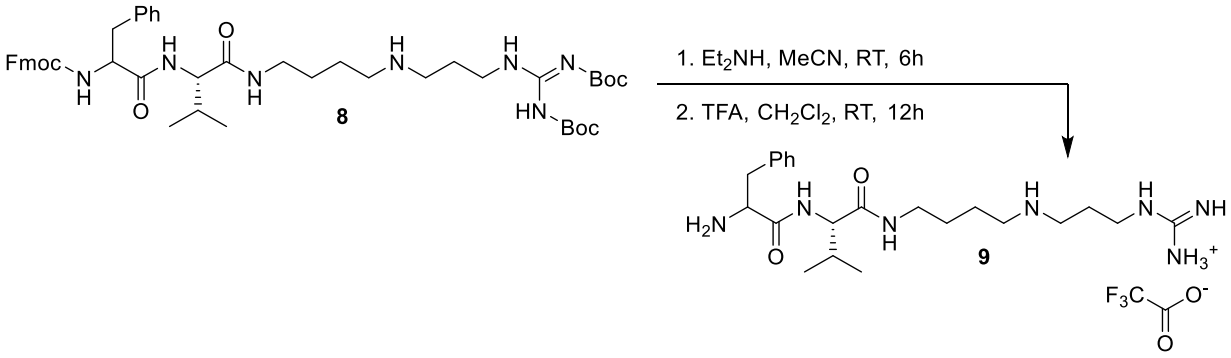

To a solution of Fmoc-(S)-Phe-(S)-Val-spermidine-*N,N'*-Di-Boc-1*H*-guanidine (**8**) (23 mg, 0.027 mmol) in 2.5 mL of MeCN, diethylamine (300µL) was added. The reaction was stirred for 6 hours at room temperature. The crude reaction mixture was concentrated under reduced pressure. Ethyl acetate was added, and the reaction mixture was concentrated again. The reaction mixture was dissolved in CH_2Cl_2 (3 mL) on ice and trifluoroacetic acid (350 µL) was added dropwise. The reaction was stirred at room temperature for 12 hours. The reaction mixture was concentrated under reduced pressure. Toluene was added and the reaction mixture was concentrated until dryness. The reaction mixture was purified by reverse-phase HPLC (Phenomenex Kinetex C18, H_2O/MeCN gradient). The final product phevamine A (**9**) was obtained as a white solid (9.8mg, 67% yield). ^{1}H NMR (400 MHz, D_2O) δ 0.79 (d, J = 6.8 Hz, 3H), 0.82 (d *J* = 6.8 Hz, 3H), 1.49 (m, 2H), 1.60 (m, 2H), 1.84 (m, 1H), 1.87 (m, 2H), 2.97−3.20 (m, 8H), 3.20 (t, *J* = 6.8 Hz, 2H), 3.87 (d, *J* = 8.4 Hz, 1H), 4.22 (t, *J* = 7.2 Hz, 1H), 7.15 (m, 2H), 7.29 (m, 3H); HRMS (EI) *m/z* $[M + H]^+$ Calculated for $C_{22}H_{40}N_7O_2$ 434.324, observed 434.323. ^{19}F NMR (400 MHz, D_2O) δ −75.67 (s).

Supplementary Tables

Name	Sequences (5' to 3')
hsv_pLIC-His_sense	**TACTTCCAATCCAATGCG**ATGTCATATCAAAAAGCAGAACCCGCTTAC
hsv_pLIC-His_anti	**TTATCCACTTCCAATGCGCTA**TCAACCACGCGCAGCTTCTGCATGC
hsv_pBBR5_sense	**GACAACAG<u>ACTAGT</u>**ATGTCATATCAAAAAGCAGAACCCG (SpeI site underlined)
hsv_pBBR5_anti	**GACAACAG<u>AAGCTT</u>** TCAACCACGCGCAGCTTC (HindIII site underlined)
hsvA_pRSF_BamHI_sense	**GACAACAG<u>GGATCC</u>**GATGTCATATCAAAAAGCAGAAC (BamHI site underlined)
hsvA_pRSF_HindIII_anti	**GACAACAG<u>AAGCTT</u>**TCAAATATAACGGTGCAGTCCT (HindIII site underlined)
hsvB_pACYC_SacI_sense	**GACAACAG<u>GAGCTC</u>**GATGCGCCCTACAAAAAAAATACTG (SacI site underlined)
hsvB_pACYC_HindIII_anti	**GACAACAG<u>AAGCTT</u>**TCACTCCTCAAACGGAGGG (HindIII site underlined)
hsvC_pCDF_BamHI_sense	**GACAACAG<u>GGATCC</u>**GATGGACAAAAATAAGCCAAACACTATTCTG A (BamHI site underlined)
hsvC_pCDF_HindIII_R	**GACAACAG<u>AAGCTT</u>**TCAACCACGCGCAGCTTCTG (HindIII site underlined)
MT1797	GTCCCGGATGAAGTAATCGGATCC
MT1881	GGGTACTGTCTAACGCCGCTATATTGACTGAAGGGGCG
MT1880	ATATAGCGGCGTTAGACAGTACCCGTCCGGGCATCCC
MT1877	**CACC**GTCTGAGGTTCTGATAGGACGGGG
MT1878	CTGCGCGACGAAATGCTCGCGGCGG
MT1967	GGGGTTCGTCCGGCCTTTCCGC
MT1968	GTGCTGATTGCGAGCACGGTCG
MT1969	GCTTCAGACCTTCCTCAAGGCG
MT1970	GTCTAATGGCTGACCGCCACTG
MT1971	AGAACCCACGTAGTGCCGGCTC
MT1972	ATGGACGCCATAGGGTGTGTAG

Table S3. Primers used for cloning of the *hsv* operon, cloning of individual *hsv* genes in *E. coli*, and generation of *hsv* knockouts. Nucleotides added for cloning are shown in bold. Restriction sites are underlined.

Insert	Plasmid	Host strain	Source
hsvA	pRSF-duet (Kan)	*E. coli* BL21	This study
hsvB	pACYC-duet (Cam)	*E. coli* BL21	This study
hsvC	pCDF-duet (Sm)	*E. coli* BL21	This study
hsvA-C	pLIC-His (Amp)	*E. coli* BL21	This study
		*P. fluorescens Pf*0-1	(11)
hrp/hrc		*EthAn Tn5 transposant of P. fluorescens Pf*0-1 (Tet)	(12)
hsvA-C	pBBR5 (Gent)	*P. fluorescens Pf*0-1	This study
		P. syringae pv. *tomato* DC3000	(2)
hrpL	pBAD (Tet)	*P. syringae* pv. *tomato* DC3000	(2)
*Tn*5::cfa6 (DC3118)		*P. syringae* pv. *tomato* DC3000	(13, 14)

Table S4. List of plasmids and strains used in this study.

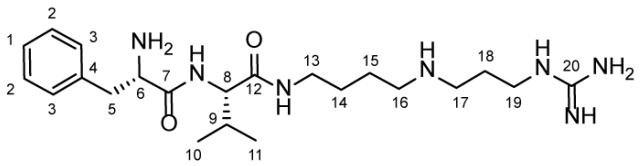

Position	δ_c	Proton	δH(J_{HH}[Hz])	HMBC
1	128.49	1-H	7.41($J_{1,2}$ = 6.9)	3
2	129.61	2-H	7.42($J_{2,1}$ = 6.9) ($J_{2,3}$ = 7.1)	2,4
3	129.86	3-H	7.26($J_{3,2}$ = 7.1)	1,3,5
4	134.07			
5	37.38	5-Ha	3.19($J_{5a,5b}$ = 14.4) ($J_{5a,6}$ = 7.5)	3,4,6,7
		5-Hb	3.23($J_{5b,5a}$ = 14.4) ($J_{5b,6}$ = 6.6)	3,4,6,7
6	54.65	6-H	4.33($J_{6,5a}$ = 7.5) ($J_{6,5b}$ = 6.6)	4,7
7	169.28			
8	60.45	8-H	3.98($J_{8,9}$ = 8.5)	7,9,10,11,12
9	30.71	9-H	1.95($J_{9,8}$ = 8.5) ($J_{9,10}$ = 6.8) ($J_{9,11}$ = 6.8)	8,10,11
10	18.49	10-3H	0.93($J_{10,9}$ = 6.8)	8,9,11
11	18.75	11-3H	0.90($J_{11,9}$ = 6.8)	8,9,10
12	172.58			
13	39.18	13-Ha	3.15($J_{13a,13b}$ = 13.3) ($J_{13a,14}$ = 7.0)	12,14,15
		13-Hb	3.29($J_{13b,13a}$ = 13.3) ($J_{13b,14}$ = 7.0)	12,14,15
14	26.02	14-2H	1.61($J_{14,13a}$ = 7.0) ($J_{14,13b}$ = 7.0) ($J_{14,15}$ = 7.6)	13,15,16
15	23.65	15-2H	1.73($J_{15,14}$ = 7.6) ($J_{15,16}$ = 7.6)	13,14,16
16	47.74	16-2H	3.10($J_{16,15}$ = 7.6)	14,15,17
17	45.29	17-2H	3.12($J_{17,18}$ = 8.0)	16,18,19
18	25.47	18-2H	2.00($J_{18,17}$ = 8.0) ($J_{18,19}$ = 6.7)	17,19
19	38.71	19-2H	3.31($J_{19,18}$ = 6.7)	17,18,20
20	157.38			

Table S5. ^{1}H (800 MHz) and ^{13}C (200 MHz) NMR spectroscopic data for phevamine A in D_2O. Chemical shifts were referenced to δ($C\underline{H}_3CO_2H$) = 2.08 ppm and δ($^{13}\underline{C}H_3CO_2H$) = 21.03. ^{13}C chemical shifts were determined via HMBC and HSQC experiments. ^{1}H, ^{1}H-*J*-coupling constants were determined from the acquired ^{1}H or dqfCOSY spectra. HMBC correlations are from the indicated proton(s) to the indicated ^{13}C atom.

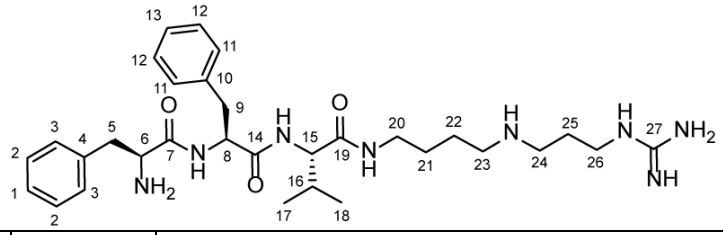

Position	δ_c	Proton	δH(J_{HH}[Hz])	HMBC
1	128.62	1-H	7.35($J_{1,2}$ = 7.0)	3
2	129.78	2-2H	7.38($J_{2,1}$ = 7.0) ($J_{2,3}$ = 7.1)	2,4
3	129.99	3-2H	7.23($J_{3,2}$ = 7.1)	1,3,5
4	134.05			
5	37.37	5-2H	3.18($J_{5,6}$ = 7.0)	3,6,7
6	54.66	6-H	4.25($J_{6,5}$ = 7.0)	4,7
7	169.12			
8	55.56	8-H	4.64($J_{8,9a}$ = 8.7) ($J_{8,9b}$ = 7.0)	7,9,13
9	37.93	9-Ha	2.99($J_{9a,9b}$ = 13.2) ($J_{9a,8}$ = 8.7)	10,11
		9-Hb	3.04($J_{9b,9a}$ = 13.2) ($J_{9b,8}$ = 7.0)	10,11
10	136.40			
11	129.78	11-2H	7.20($J_{11,12}$ = 7.5)	9,11,13
12	129.35	12-2H	7.34($J_{12,11}$ = 7.5) ($J_{12,13}$ = 7.0)	10,12
13	127.84	13-H	7.30($J_{13,12}$ = 7.0)	11
14	172.18			
15	60.39	15-H	3.85($J_{15,16}$ = 8.4)	14,16,18,19
16	30.81	16-H	1.91($J_{16,15}$ = 8.4) ($J_{16,17}$ = 6.8) ($J_{16,18}$ = 6.8)	18
17	18.87	17-3H	0.87($J_{17,16}$ = 6.8)	15,16,18
18	18.72	18-3H	0.91($J_{18,16}$ = 6.8)	15,16,17
19	172.85			
20	39.20	20-Ha	3.08($J_{20a,20b}$ = 13.5) ($J_{20a,21}$ = 7.0)	19,21,22
		20-Hb	3.18($J_{20b,20a}$ = 13.5) ($J_{20b,21}$ = 7.0)	19,21,22
21	26.07	21-2H	1.54($J_{21,20a}$ = 7.0) ($J_{21,20b}$ = 7.0) ($J_{21,22}$ = 7.0)	20,23
22	23.69	22-2H	1.67($J_{22,21}$ = 7.0) ($J_{22,23}$ = 7.8)	20,23
23	47.80	23-2H	3.05($J_{23,22}$ = 7.8)	21,22,24
24	45.35	24-2H	3.09($J_{24,25}$ = 7.8)	23,25,26
25	25.56	25-2H	1.98($J_{25,24}$ = 7.8) ($J_{25,26}$ = 7.0)	24,26
26	38.80	26-2H	3.28($J_{26,25}$ = 7.0)	24,25,27
27	157.47			

Table S6. ^{1}H (800 MHz) and ^{13}C (200 MHz) NMR spectroscopic data for phevamine B in D_2O. Chemical shifts were referenced to δ($C\underline{H}_3OH$) = 3.34 ppm and δ($^{13}\underline{C}H_3OH$) = 49.50. ^{13}C chemical shifts were determined via HMBC and HSQC experiments. ^{1}H, ^{1}H-*J*-coupling constants were determined from the acquired ^{1}H or dqfCOSY spectra. HMBC correlations are from the indicated proton(s) to the indicated ^{13}C atom.

Supplementary Figures

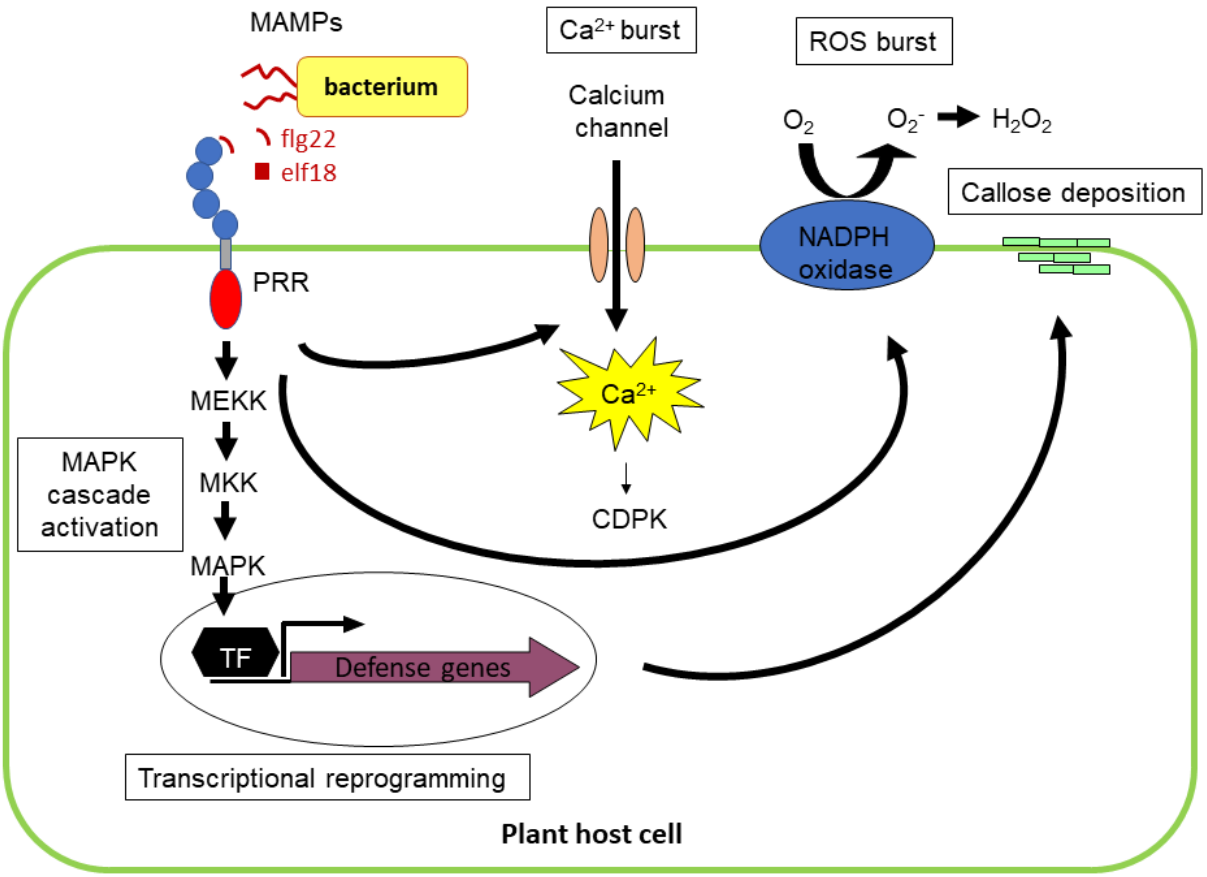

Figure S1. Plant immune response schematic. Diagram showing several MAMP-induced immune responses in a plant host cell. Upon elicitation by a MAMP, a plant cell may induce MAPK cascade activation, transcriptional reprogramming, calcium burst, ROS burst, synthesis of various secondary metabolites, and callose deposition. Collectively, these responses are sufficient to suppress pathogen proliferation. MAMP: microbe-associated molecular pattern, PRR: pathogen recognition receptor, TF: transcription factor, MEKK: mitogen-activated protein (MAP) kinase kinase kinase, MKK: MAP kinase kinase, MAPK: MAP kinase, CDPK: calcium-dependent protein kinase, ROS: reactive oxygen species.

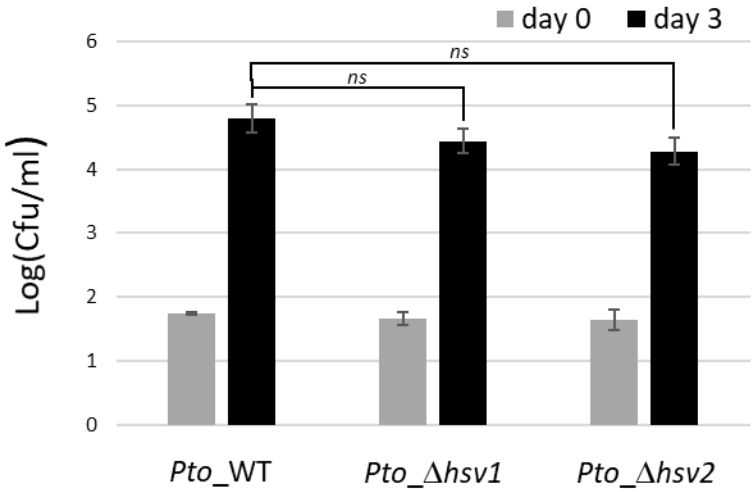

Figure S2. *Pto*_Δ*hsv* mutants do not display significantly reduced virulence on *A. thaliana*. Bacteria were counted after recovery from *Pto*-wildtype and *Pto*_Δ*hsv* mutants on *A. thaliana* seedlings. The experiment was repeated twice with similar results. The mutants in both experiments displayed slightly reduced growth but this was not statistically significant (Student's *t*-tests). ns: non significant. Error bars represent ± standard error.

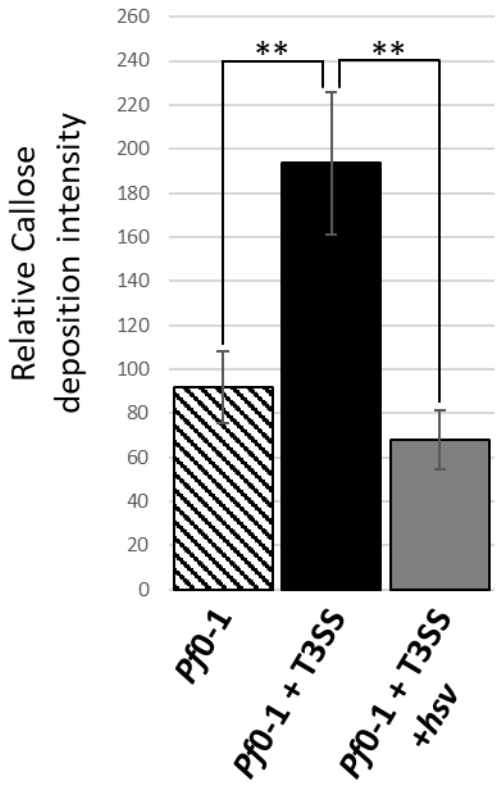

Figure S3. The *hsv* operon suppresses callose deposition in *A. thaliana* induced by components encoded by the T3SS locus. Leaves of 4-week-old *A. thaliana* were infiltrated with the *P. fluorescens* strains noted at bottom and stained with aniline blue, ~20 h post infiltration. **, *p*-value ≤ 0.01; *t*-test. Error bars represent standard errors. This experiment was repeated 3 times with similar results.

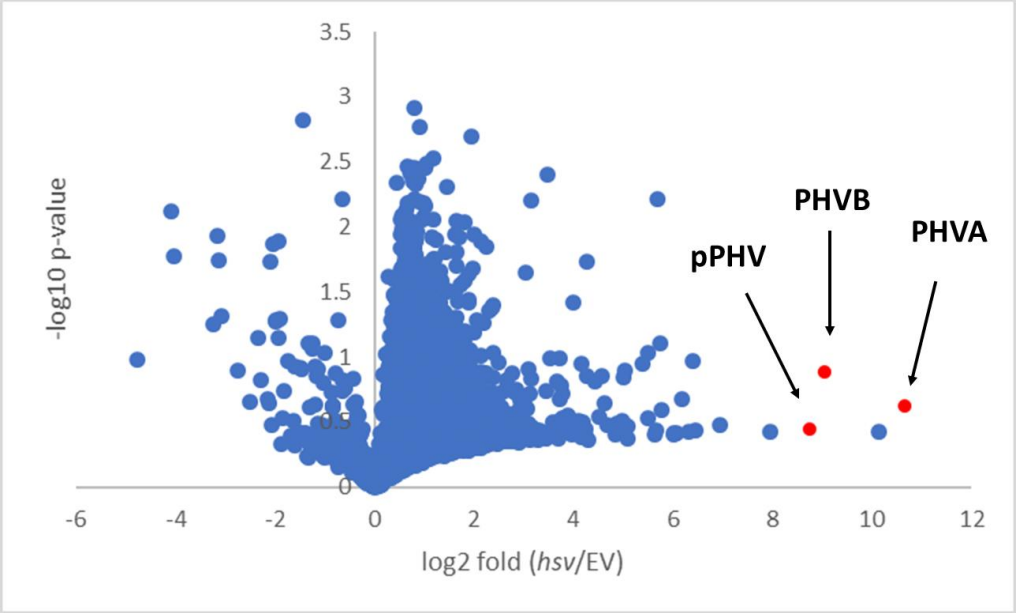

Figure S4. Identification of phevamines by comparative metabolomics. The LC-MS metabolic profiles are compared between the extract of *E. coli* overexpressing *hsv* and *E. coli* control containing the empty vector. The fold change ($\log_2$) for each metabolite is plotted against the *p*-value ($\log_{10}$) for that metabolite. Data points for prephevamine (pPHV), phevamine A (PHVA), and phevamine B (PHVB) are highlighted in red. The average fold change is very large for prephevamine (430 fold increase), phevamine A (1600 fold increase), and phevamine B (540 fold increase) comparing *hsv* overexpression and the empty vector control. When the fold change for a metabolite is large, the level in each sample tends to vary more. The relatively large *p*-values for these metabolites may be due to variable protein levels upon overexpression.

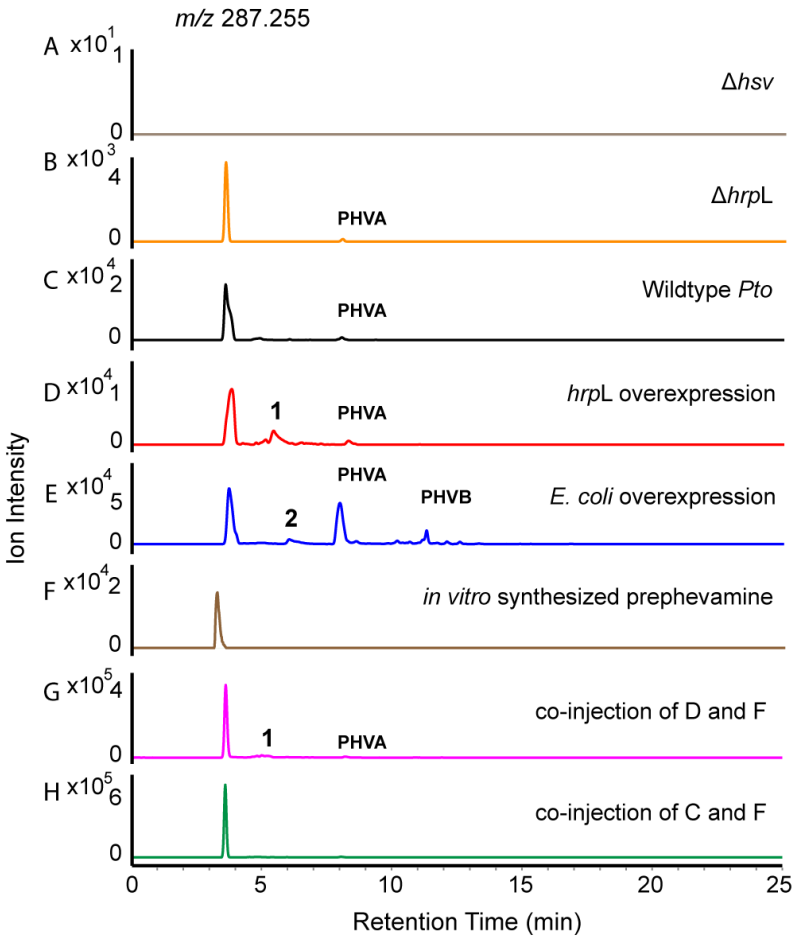

Figure S5. Production of prephevamine by different bacterial strains. Extracted ion chromatograms are shown for prephevamine (*m/z*, 287.255) detected in the extracts of each bacterial strain. The retention time of prephevamine is approximately 3.8 minutes. Prephevamine is not produced by *Pto*Δ*hsv* (*hsv* deletion mutant in *Pto*) (gray). Prephevamine is produced by *Pto*Δ*hrpL* (*hrpL* deletion mutant in *Pto*) (orange), wildtype *Pto* (black), *Pto* pBAD:*hrpL* overexpression (red), and *E. coli* overexpressing the *hsv* operon (blue). Prephevamine is also produced in the *in vitro* enzymatic reaction and was purified by HPLC (brown). The *in vitro* purified standard was co-injected with the *hrpL* overexpression extract (pink) and the wildtype *Pto* extract (green), both showing a single peak for prephevamine. In (*D*), (*E*), and (*G*), the additional prephevamine peaks result from in-source fragmentation of phevamine A or phevamine B as labeled. Lowering the fragmentor voltage reduced these in-source fragmentation peaks. Two metabolites from extractions, 1 and 2, are structurally unrelated to prephevamine based on LC/MS/MS analysis.

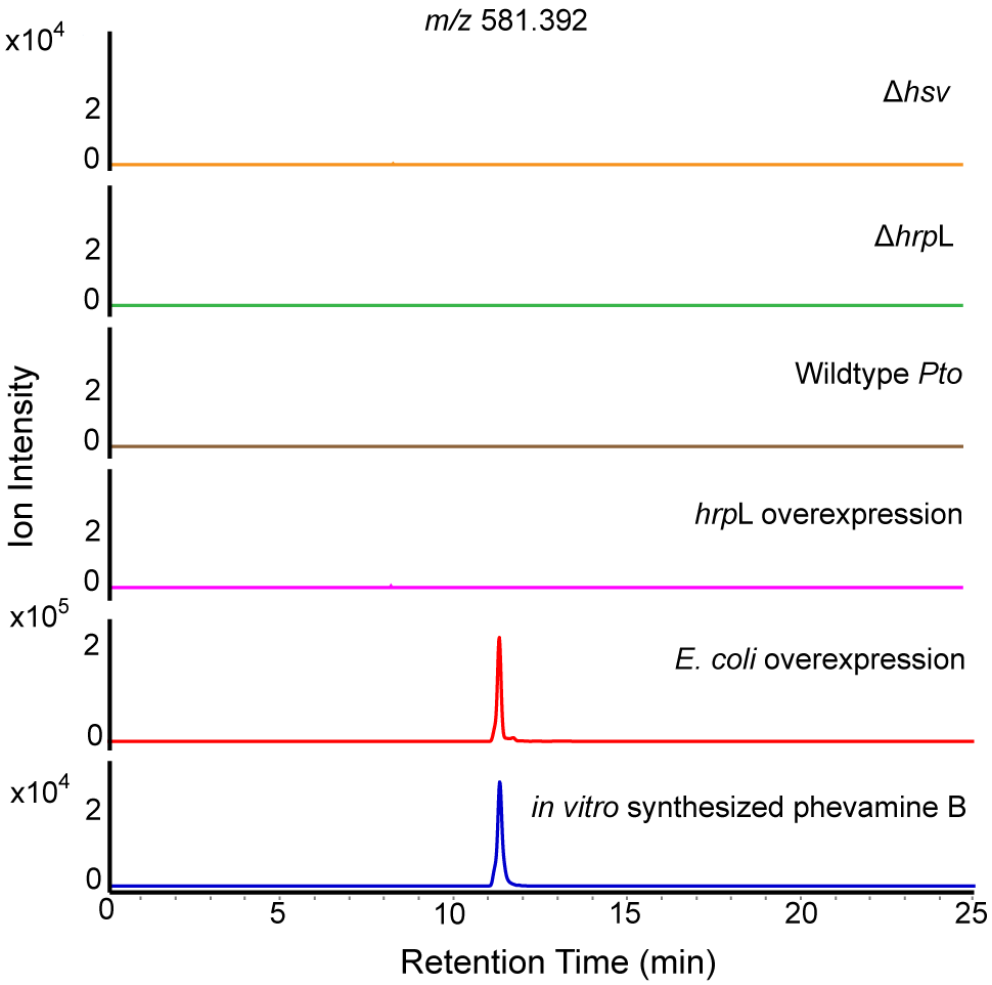

Figure S6. Production of phevamine B by different bacterial strains. Extracted ion chromatograms are shown for phevamine B (*m/z*, 581.392). Phevamine B is not produced by *Pto*Δ*hsv* (*hsv* deletion mutant in *Pto*) (orange), *Pto*Δ*hrpL* (*hrpL* deletion mutant in *Pto*) (green), wildtype *Pto* (brown), or *Pto* pBAD:*hrpL* overexpression (pink). Phevamine B is only detected in *E. coli* overexpressing *hsv* (red) and *in vitro* enzymatic reaction (blue).

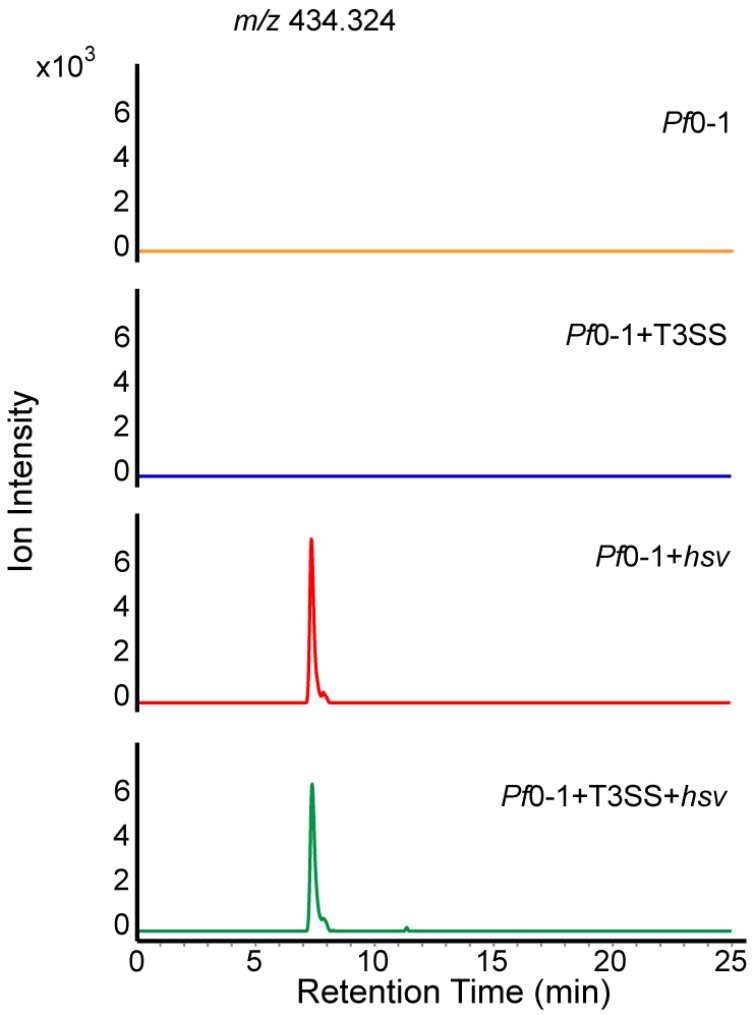

Figure S7. Phevamine A production in *P. fluorescens Pf*0-1 is independent of T3SS. Extracted ion chromatograms of phevamine A (*m/z* 434.324) are shown. Phevamine A is detected in both *Pf*0-1 strains expressing *hsv, Pf*0-1+T3SS+*hsv* (green) and *Pf*0-1+*hsv* (red), indicating that the T3SS is not required for the secretion of phevamine A. Phevamine A is not detected in the culture extracts of control strains without *hsv*, *Pf*0-1+T3SS (blue) or *Pf*0-1 (orange).

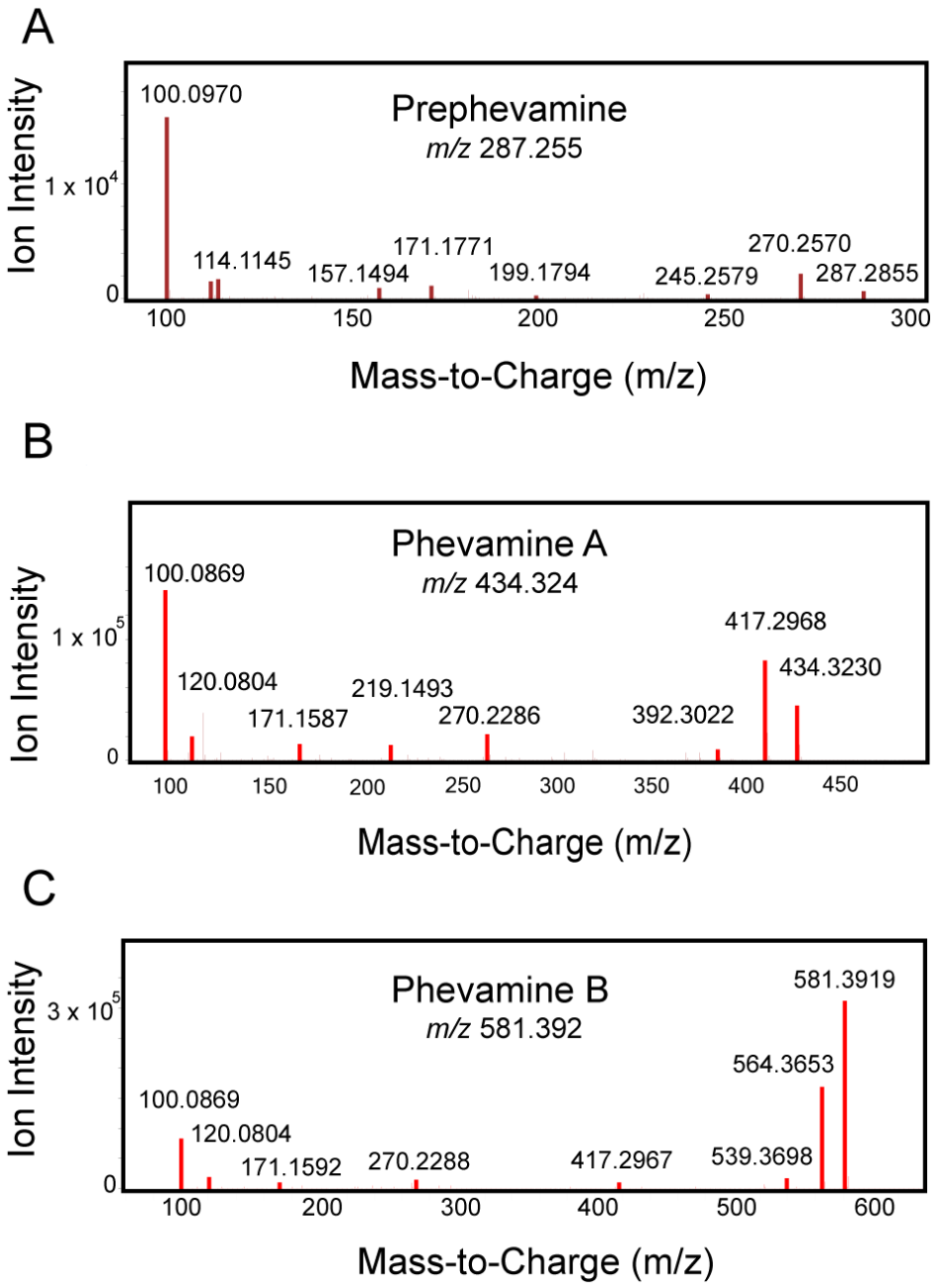

Figure S8. Structural analyses of prephevamine and phevamines by tandem mass spectrometry (LC-MS/MS). *(A)* MS/MS spectrum of prephevamine (*m/z* 287.255). *(B)* MS/MS spectrum of phevamine A (*m/z* 434.324). (*C)* MS/MS spectrum of phevamine B (*m/z* 581.392).

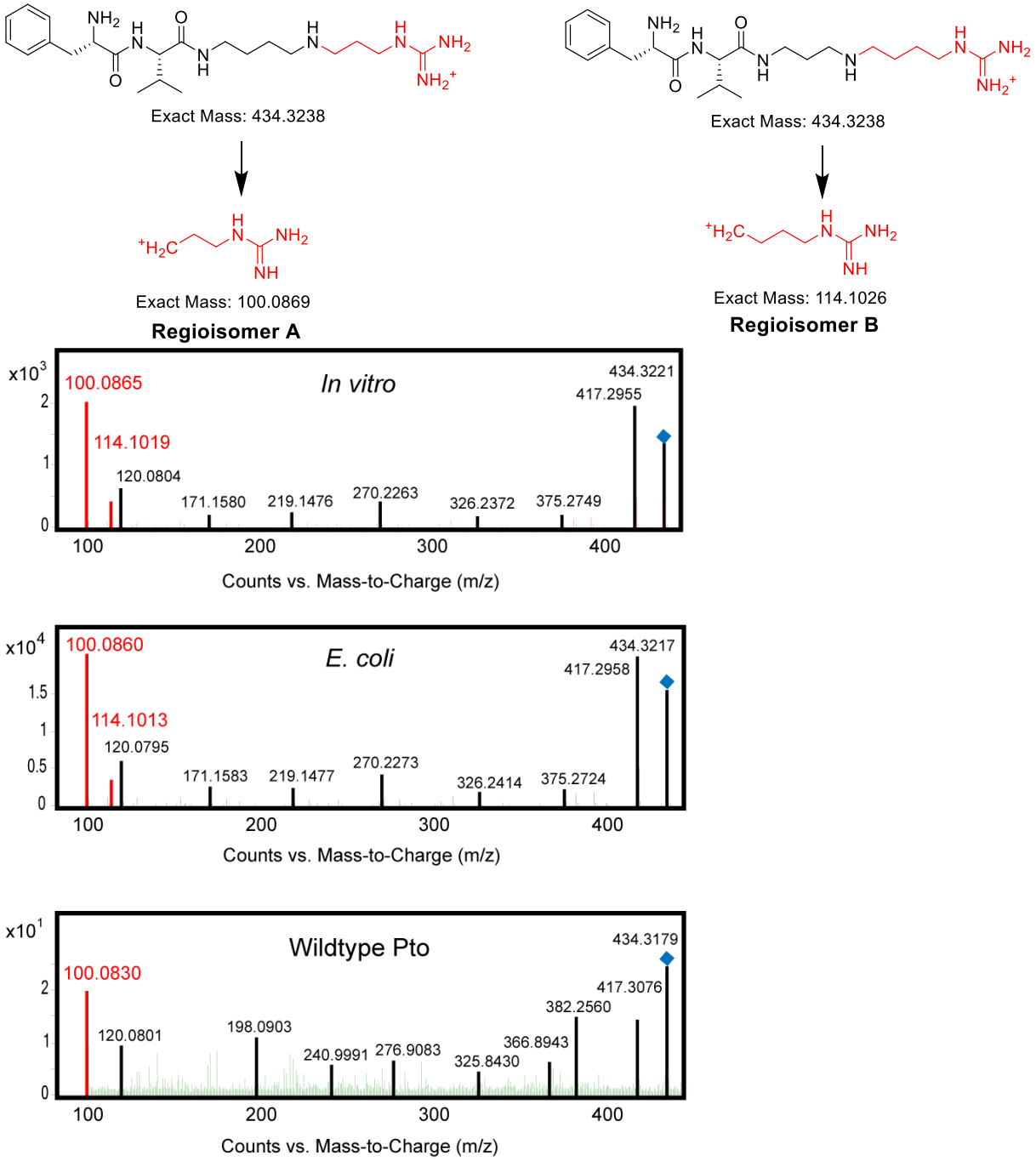

Figure S9. Identification of the regioisomers of phevamine A by LC-MS/MS. A 100 *m/z* fragment is unique to the amidinotransfer product on the propylamine end of spermidine (regioisomer A), and a 114 *m/z* fragment is unique to the amidinotransfer product on the butylamine end of spermidine (regioisomer B). Both isomers are detected from the *in vitro* reaction and *E. coli* overexpression. In culture extracts of wildtype *Pto*, only regioisomer A was detected.

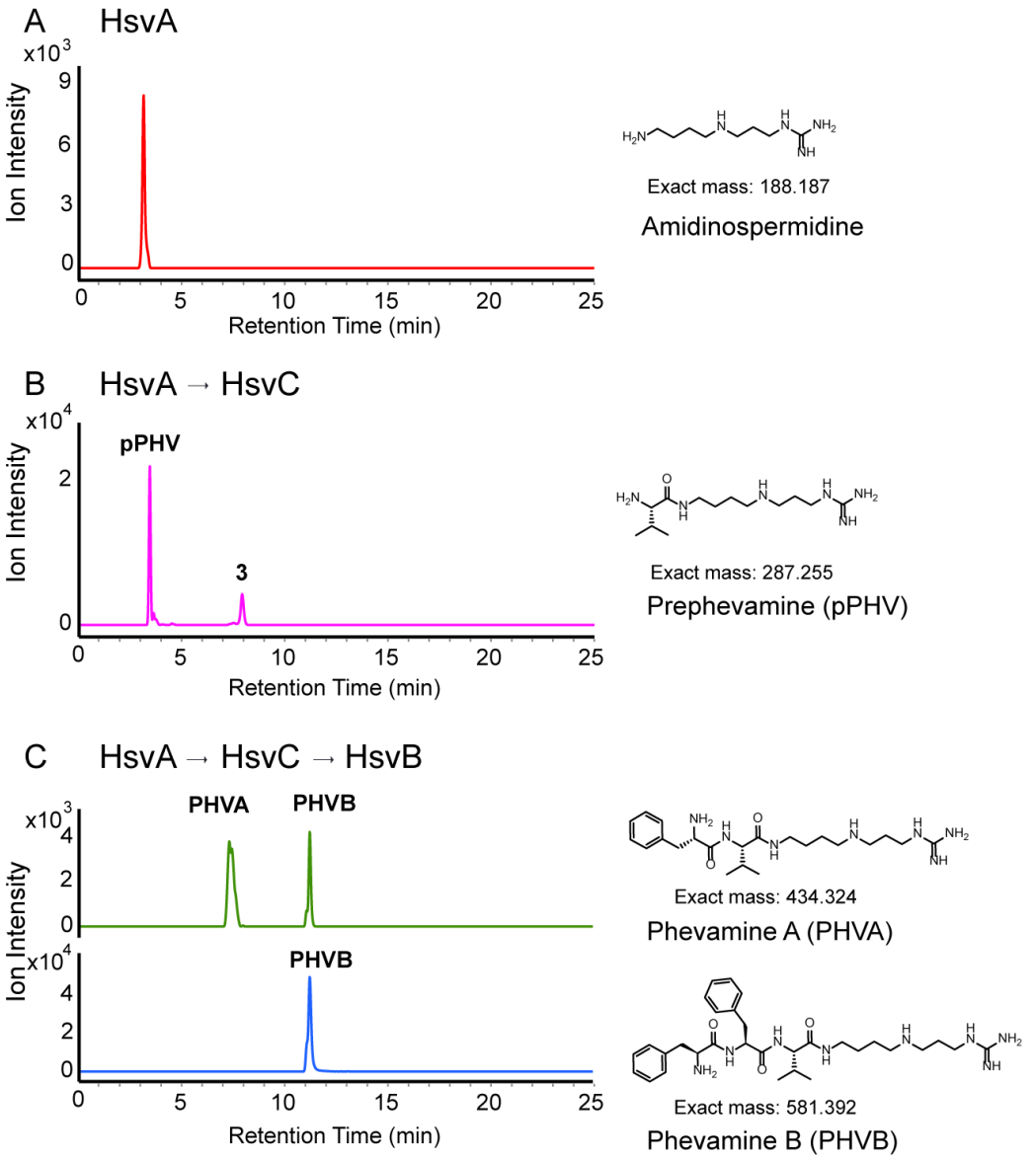

Figure S10. Production of phevamines and detection of pathway intermediates by sequential *in vitro* enzymatic assays. Extracted ion chromatograms are shown for *(A)* amidinospermidine (*m/z* 188.187) from HsvA reaction, *(B)* prephevamine (*m/z* 287.255) from HsvA reaction followed by HsvC reaction, and *(C)* phevamine A (*m/z* 434.324, green) and phevamine B (*m/z* 581.392, blue) from sequential reactions of HsvA, HsvC, and HsvB. In (*B*), the second small peak for prephevamine comes from in-source fragmentation of Compound 3, the mass of which corresponds to Val-Val-Val-amidinospermidine, an *in vitro* byproduct of the HsvC reaction. In (*C*), the second peak for phevamine A is the result of in-source fragmentation of phevamine B.

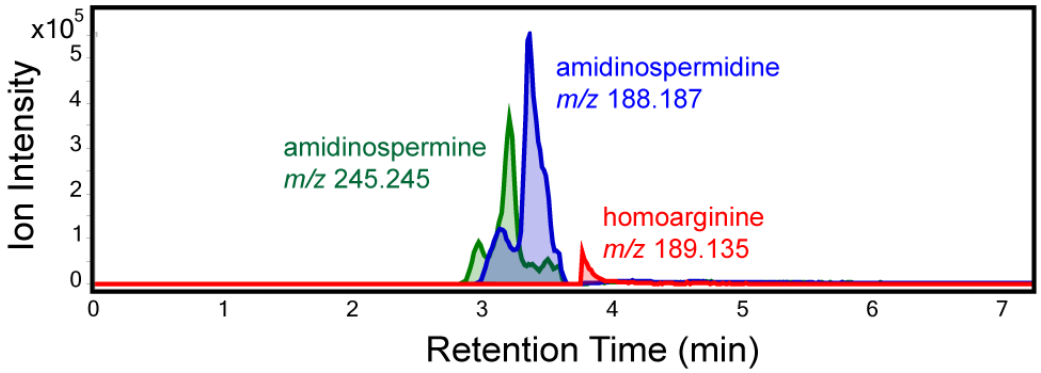

Figure S11. *In vitro* reconstitution of HsvA activity. HsvA was incubated with spermine, spermidine, and L-lysine as the acceptor of the amidino group and L-arginine as the donor of the amidino group. Extracted ion chromatograms are shown for amidinospermidine (*m/z* 188.187), amidinospermine (*m/z* 245.245), and homoarginine (*m/z* 189.135), which are the amidinotransfer products catalyzed by HsvA for spermidine, spermine, and arginine, respectively.

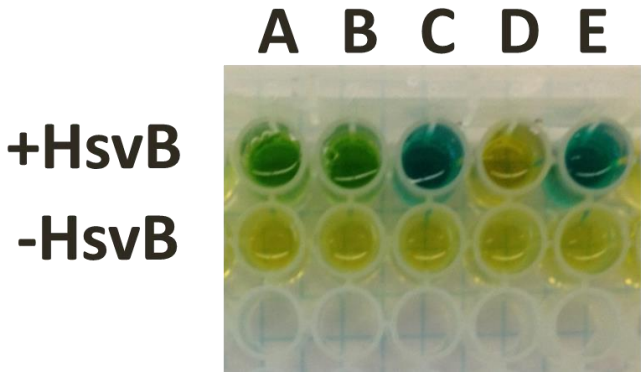

Figure S12. HsvB activates L-Phe as the preferred substrate. Several pairs of amino acids were incubated with HsvB and the released inorganic phosphate (P_i) was measured using the P_iColorLock assay described in the Methods. The amino acid pairs are (A) L-Ser and L-Orn, (B) L-Ala and L-Lys, (C) L-Ala and L-Phe, (D) L-Arg and L-Trp, and (E) 2x L-Phe. The assays containing L-Phe ((C) and (E)) produced the most P_i, indicating that L-Phe is the preferred substrate for HsvB.

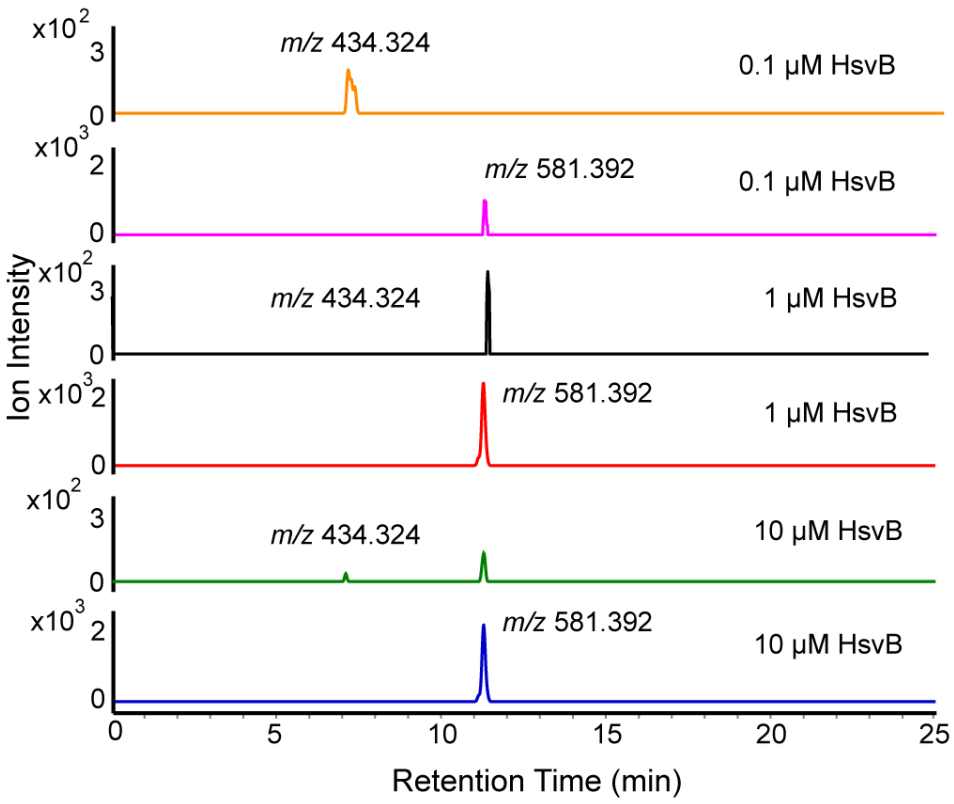

Figure S13. Production of phevamine A and B depends on HsvB concentration. Reaction mixtures containing 100 μM pPHV, 20 μM Phe, and varying amounts of HsvB were incubated at room temperature for 2 hours. As the concentration of HsvB increased, the amount of phevamine B (*m/z* 581.392) increased (pink, red, and blue). The ratio of phevamine A (*m/z* 434.324) (orange, black and green) to phevamine B is the highest at low concentration of HsvB. The peak around 11 minute retention time in phevamine A traces is a result of in-source fragmentation of phevamine B.

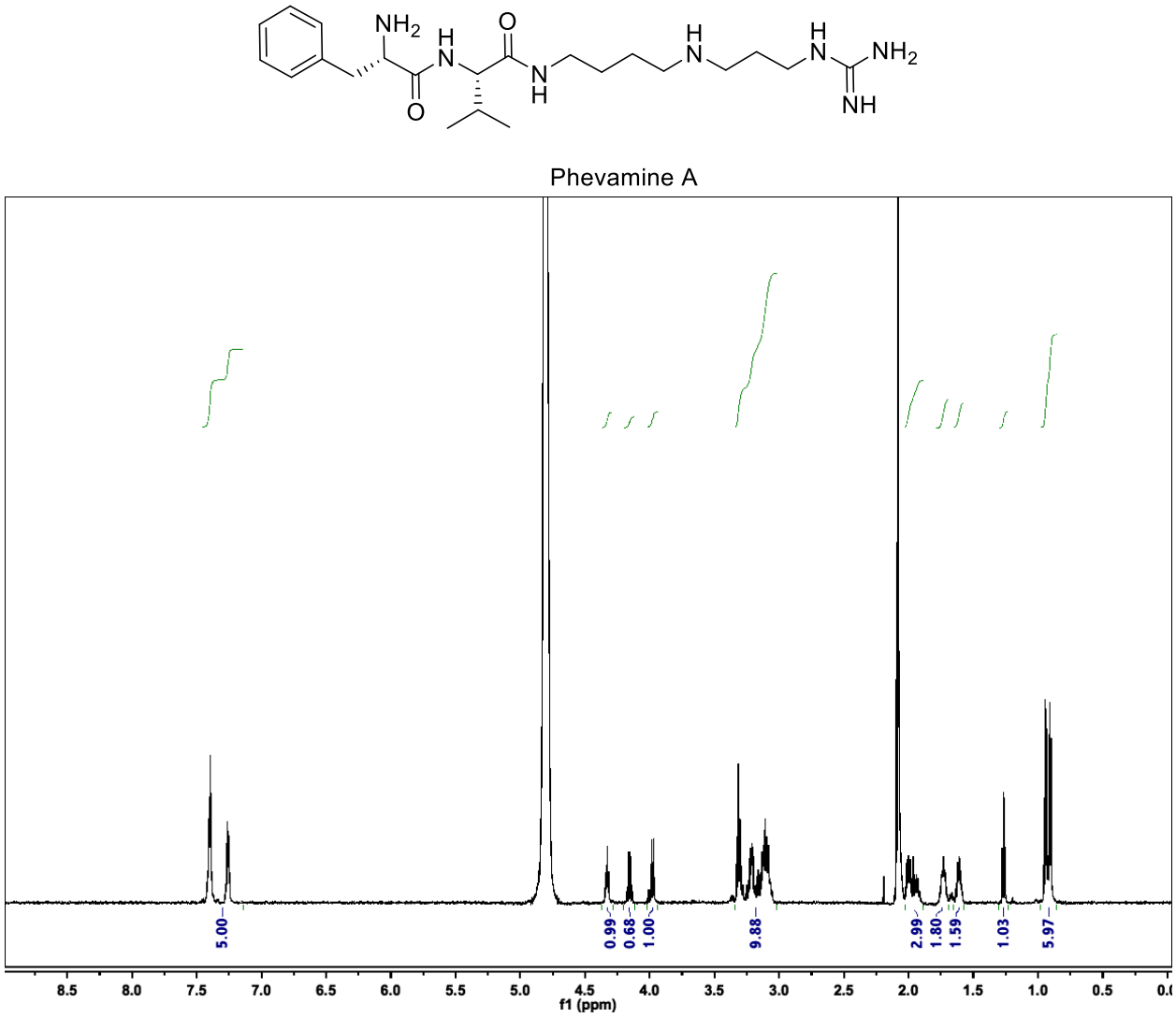

Figure S14. ^{1}H NMR (600 MHz) of *in vitro* synthesized and purified phevamine A. Spectrum acquired in D_2O.

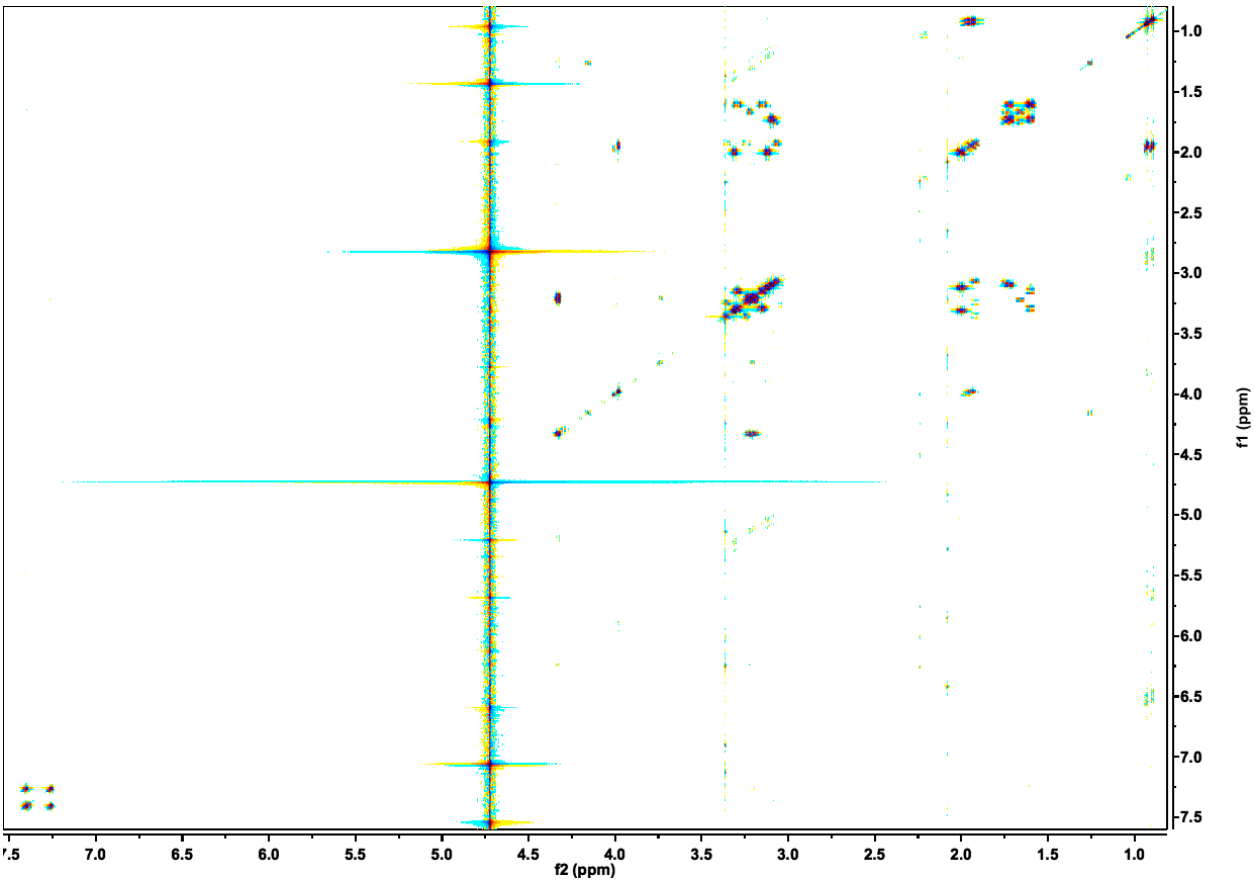

Figure S15. (^{1}H,^{1}H)-dqfCOSY spectrum (800 MHz) of *in vitro* synthesized and purified phevamine A. Spectrum acquired in CD_3OD.

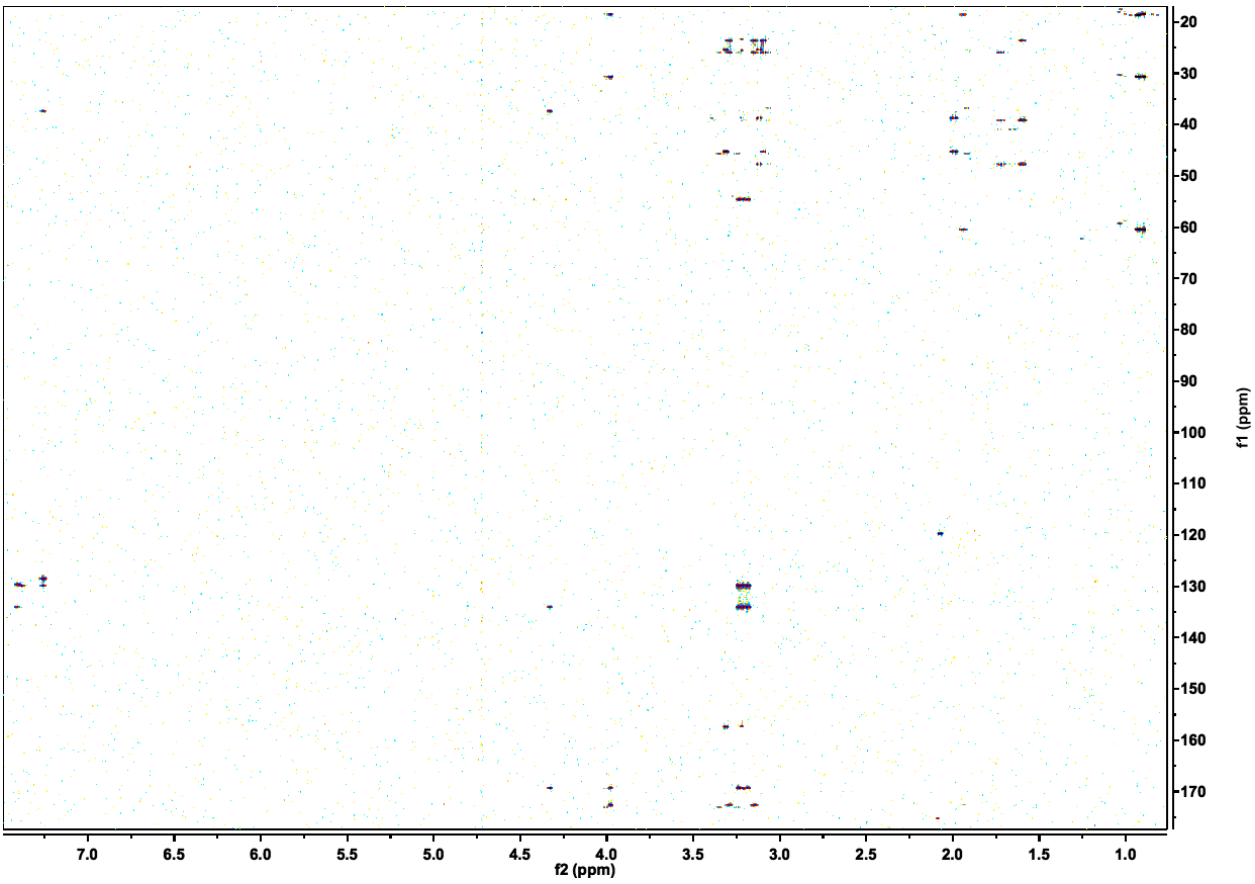

Figure S16. (^{1}H,^{13}C)-HMBC spectrum (800 MHz) of *in vitro* synthesized and purified phevamine A. Spectrum acquired in CD_3OD.

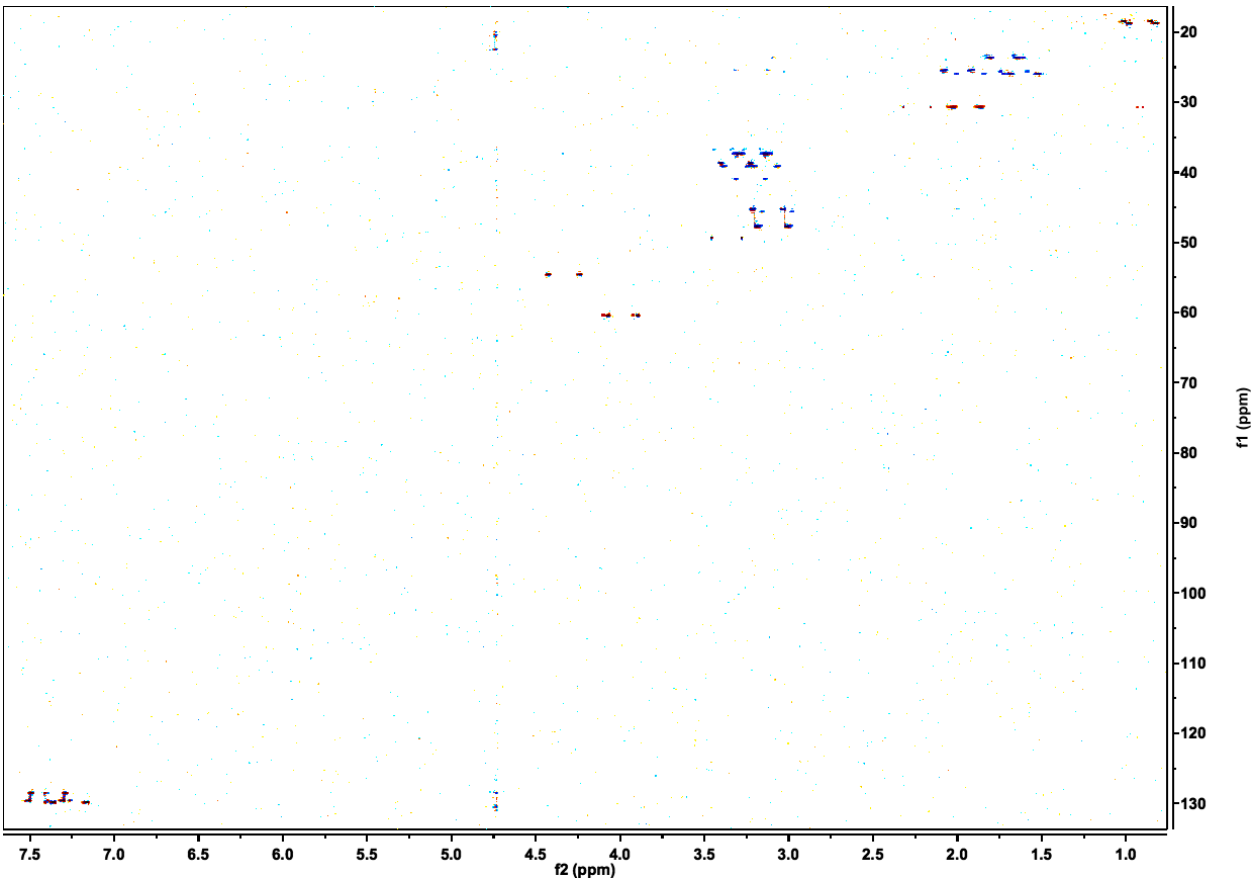

Figure S17. (^{1}H,^{13}C)-coupled-HSQC spectrum (800 MHz) of *in vitro* synthesized and purified phevamine A. Spectrum acquired in CD_3OD.

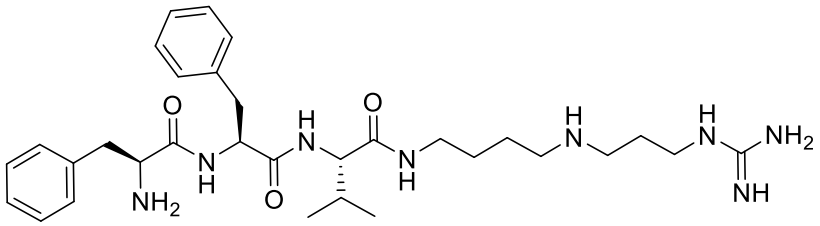

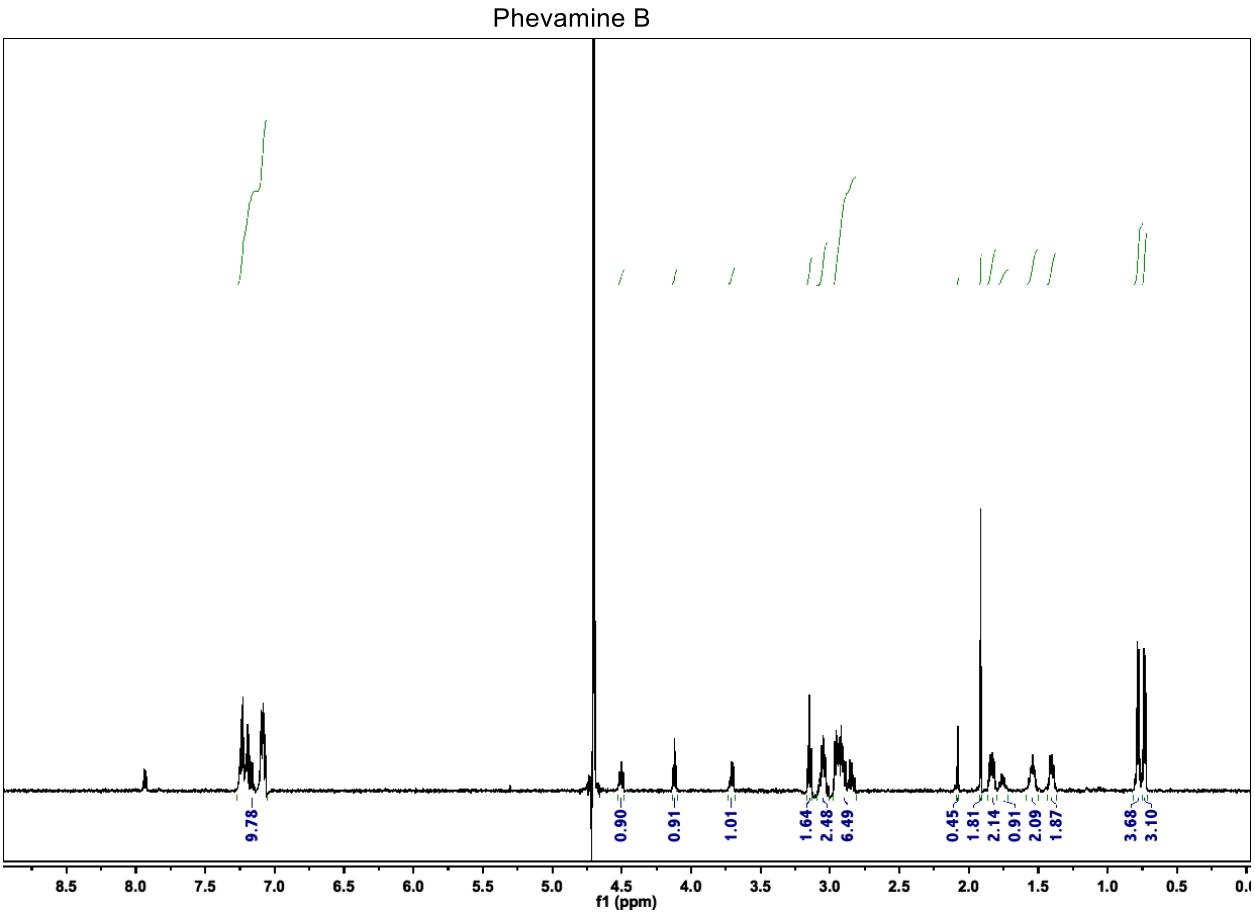

Figure S18. ^{1}H NMR (600 MHz) of *in vitro* synthesized and purified phevamine B. Spectrum acquired in CD_3OD.

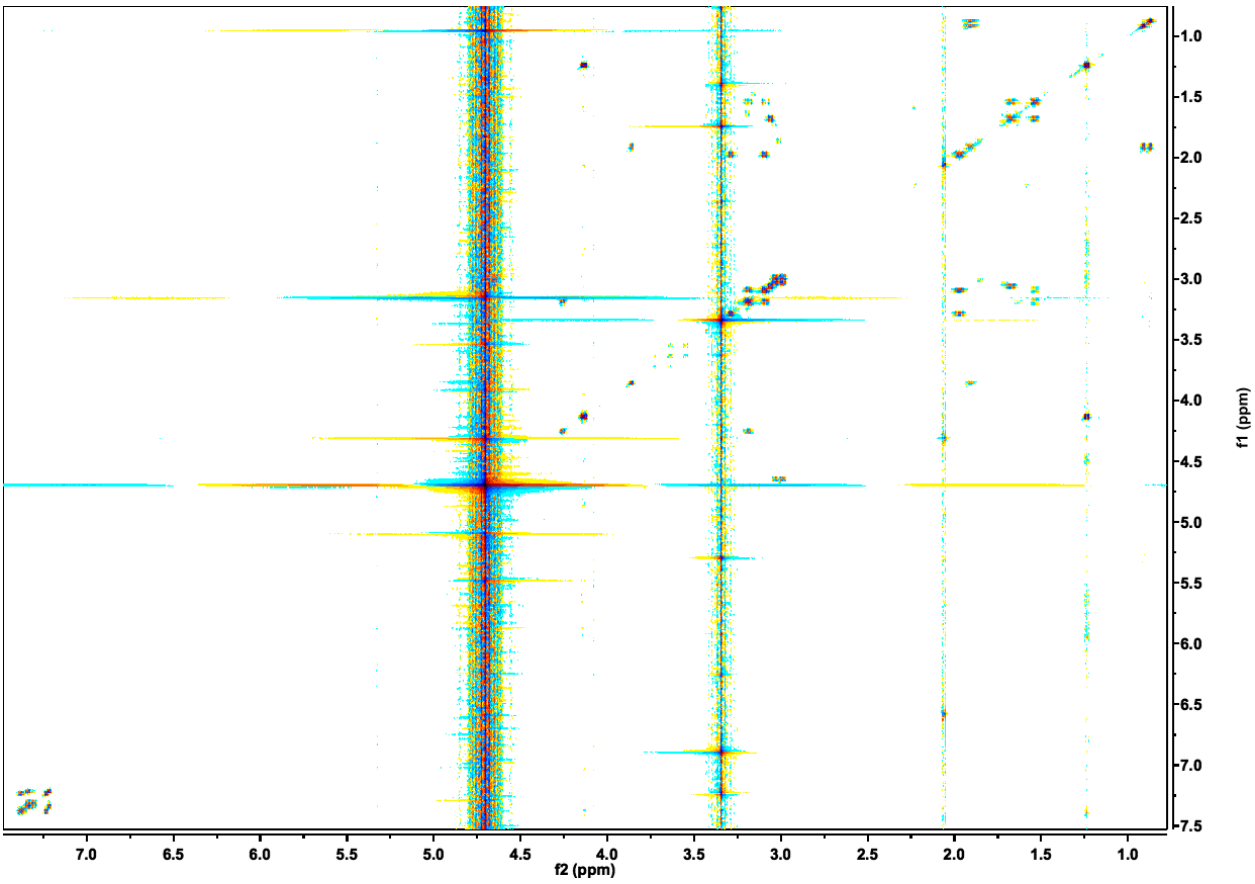

Figure S19. (^{1}H,^{1}H)-dqfCOSY spectrum (800 MHz) of *in vitro* synthesized and purified phevamine B. Spectrum acquired in CD_3OD.

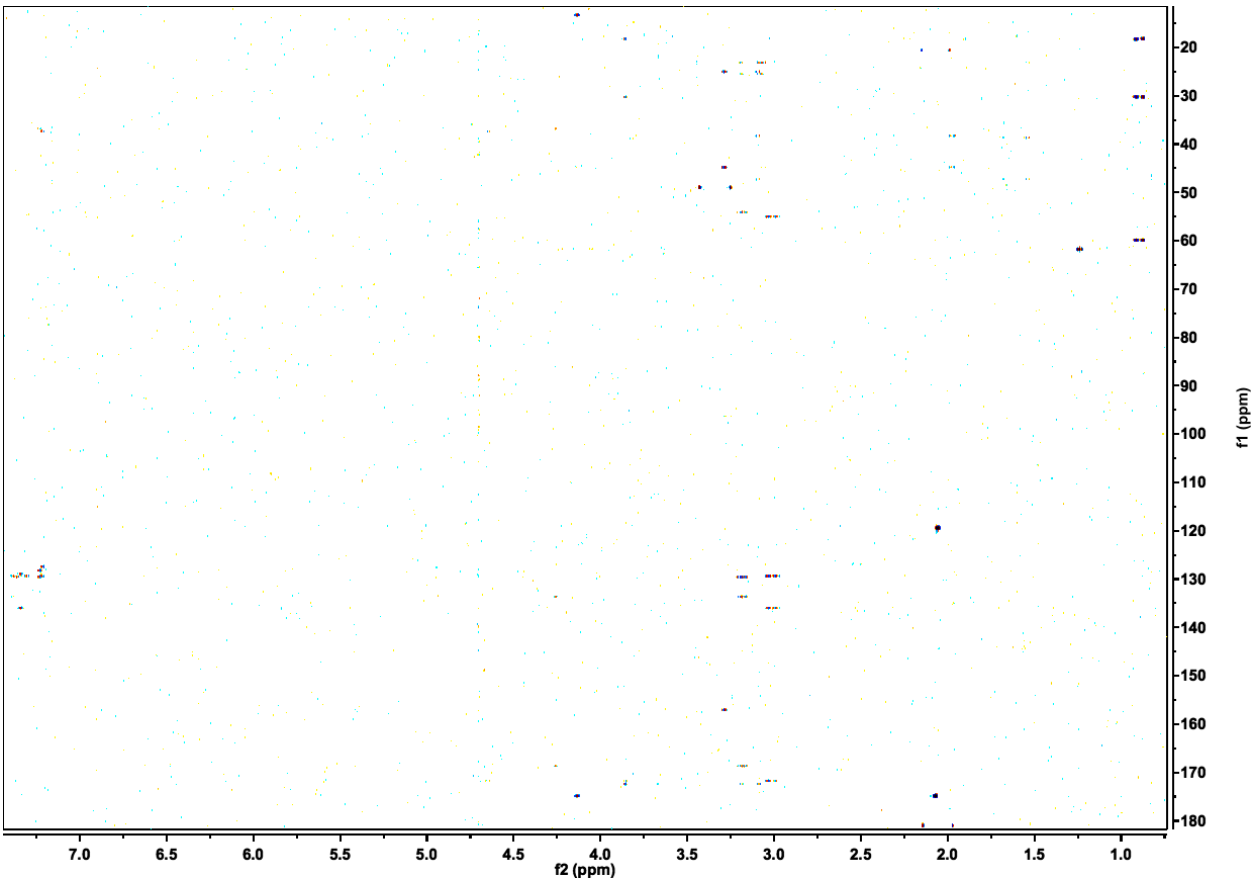

Figure S20. (^{1}H,^{13}C)-HMBC spectrum (800 MHz) of *in vitro* synthesized and purified phevamine B. Spectrum acquired in CD_3OD.

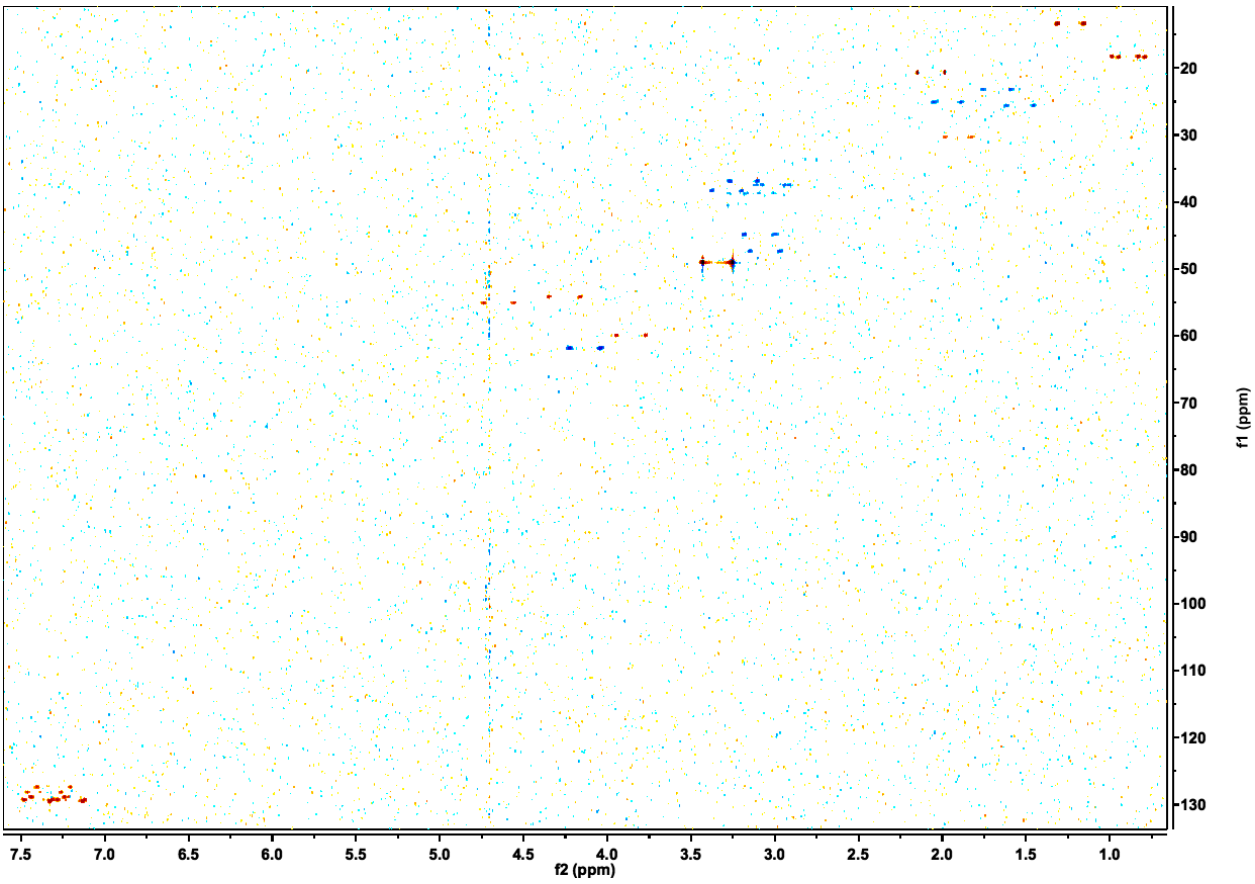

Figure S21. (^{1}H,^{13}C)-coupled-HSQC spectrum (800 MHz) of *in vitro* synthesized and purified phevamine B. Spectrum acquired in CD_3OD.

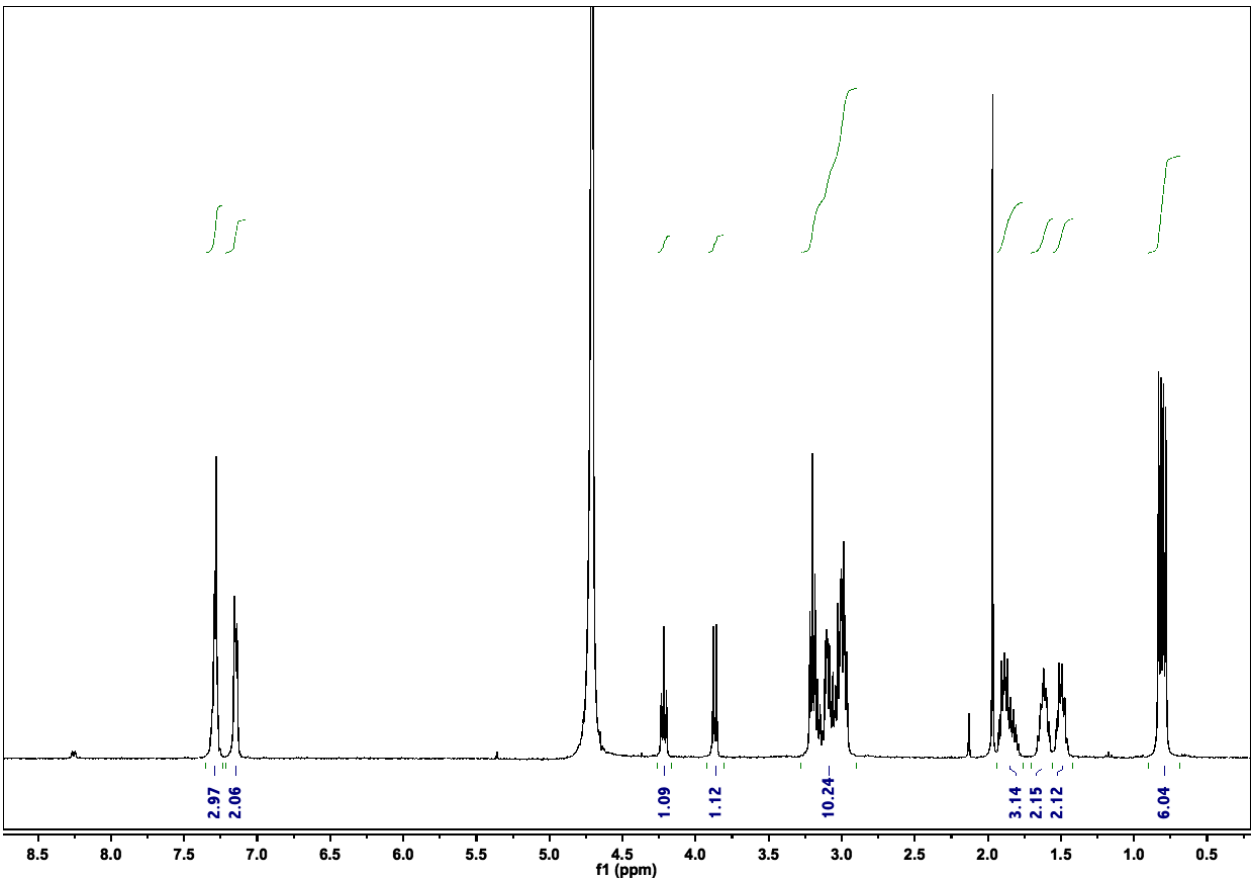

Figure S22. ^{1}H NMR (400 MHz) of the phevamine A synthetic standard (9). Spectrum acquired in D_2O.

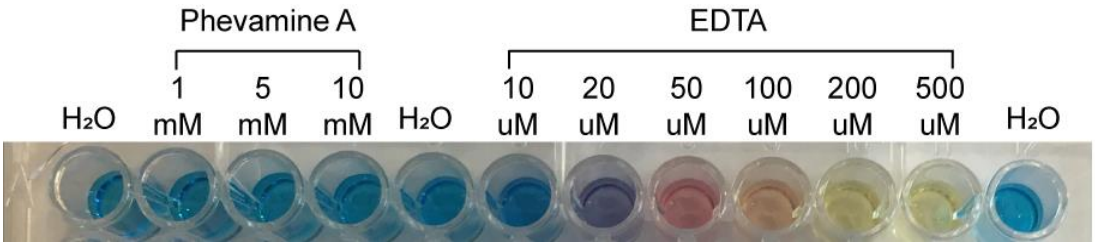

Figure S23. Iron binding activity of phevamine A. The ability of phevamine A to bind iron was tested and compared to EDTA standards using a chromeazurol S (CAS) assay. Upon binding of ferric iron, the chromeazurol S dye changes color from blue to yellow. No color change was observed for phevamine A at a concentration of up to 10 mM, thus it is unlikely that phevamine A acts as a siderophore to bind ferric iron.

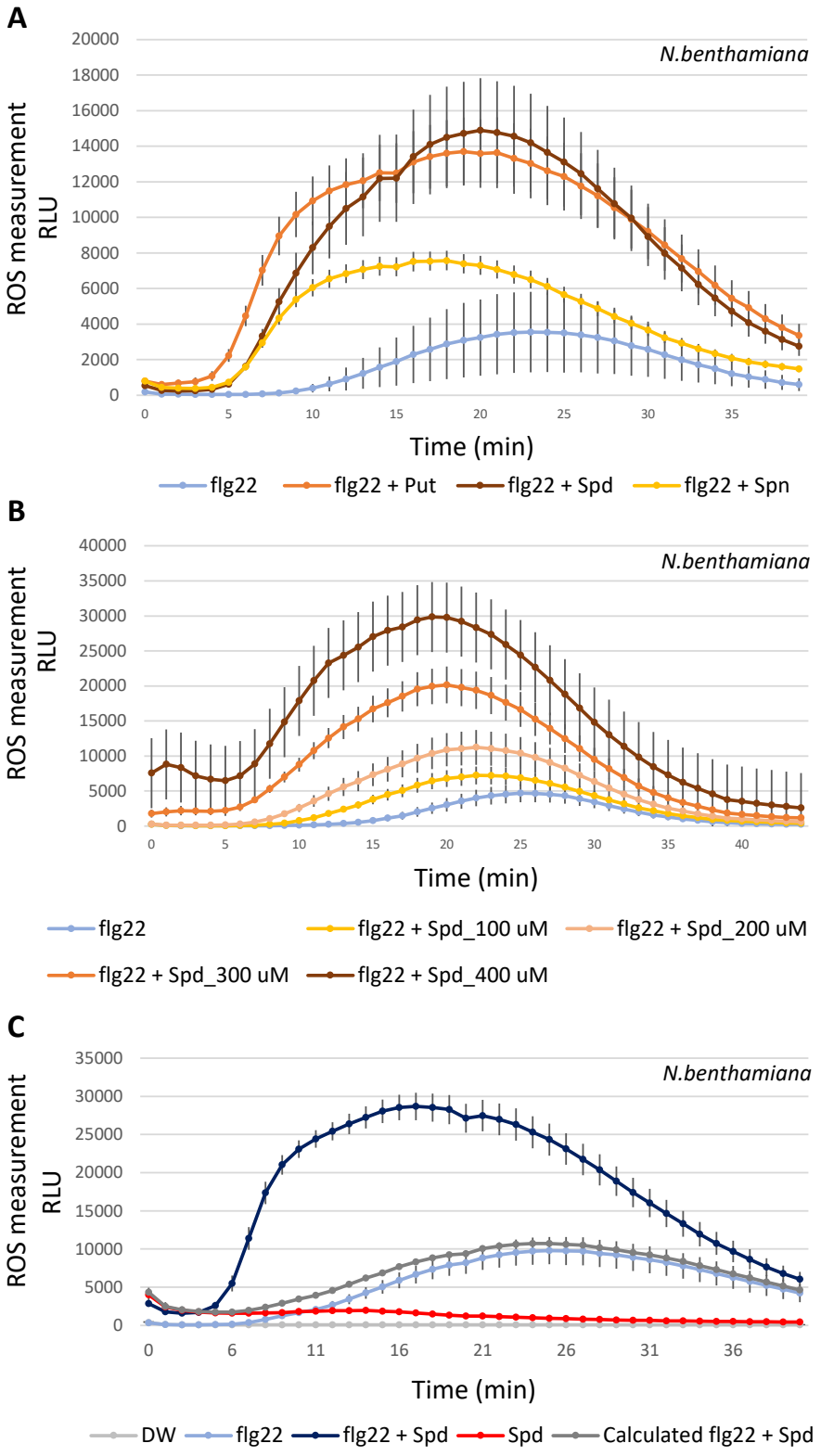

Figure S24. Polyamines enhance the flg22-induced ROS burst in *N. benthamiana*. *(A)* Various polyamines potentiate the flg22-induced ROS burst. Leaf disks were

challenged with 10 nM of flg22 with or without polyamines at 400 µM. Put: putrescine, Spd: spermidine, and Spn: spermine. *(B)* Dose-dependent effect of spermidine on the flg22-induced ROS burst. Leaf disks were challenged with 10 of nM flg22 and various concentrations of spermidine. *(C)* The increase of the flg22-induced ROS burst by spermidine is not due to an additive effect. Leaf disks were treated with distilled water (DW), 10 nM of flg22, 10 nM of flg22 with 400 µM of spermidine, or 400 µM of spermidine only. Experiments presented in panels (*A*) and (*C*) were performed more than 3 times with similar results. The experiment presented in panel (*B*) was done twice with similar results. Error bars represent standard errors.

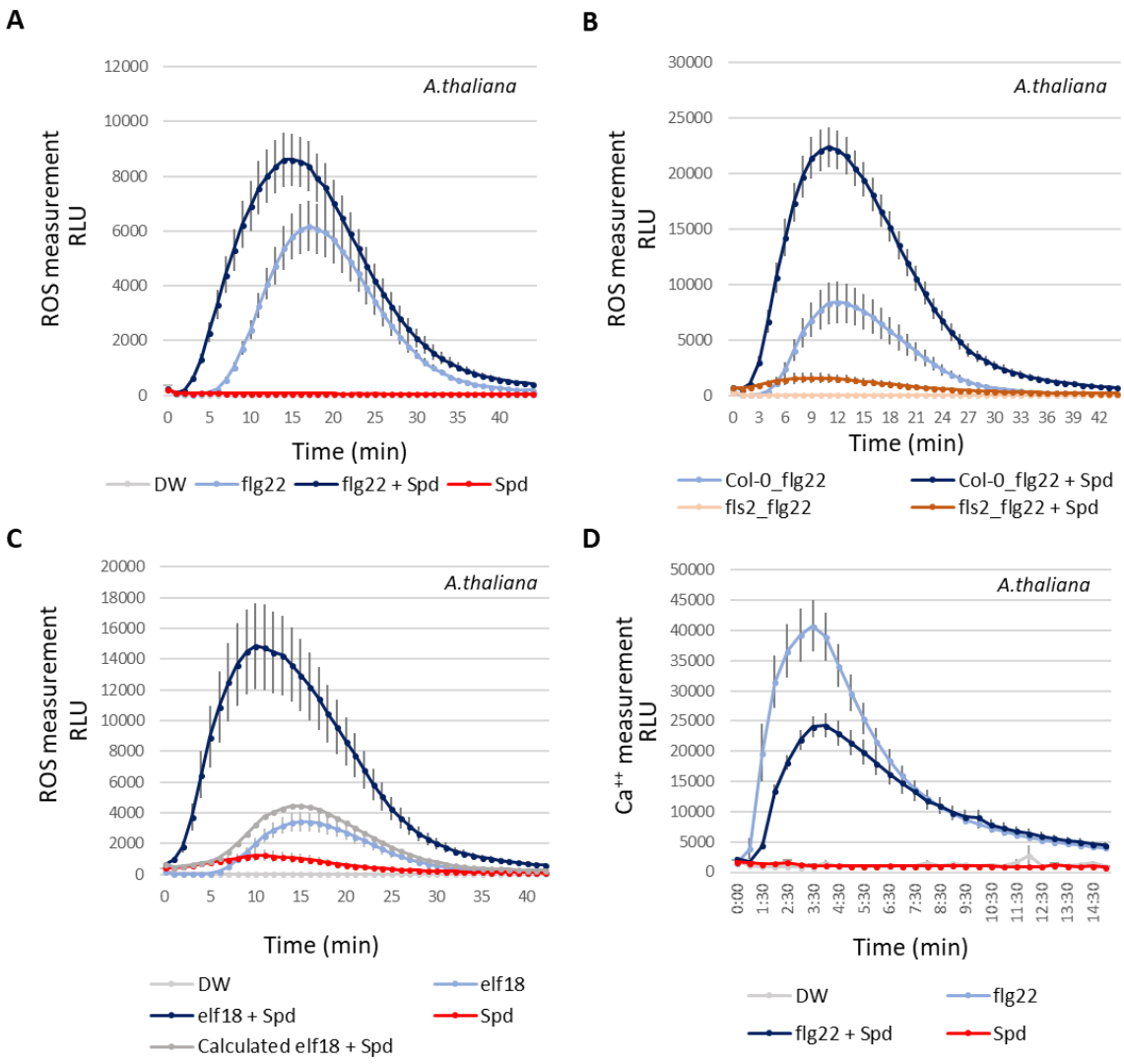

Figure S25. Effect of spermidine on early MTI responses in *A. thaliana*. (*A*) Spermidine potentiates the flg22-induced ROS burst. Leaf disks were treated with distilled water (DW), flg22 at 10 nM, flg22 with spermidine at 300 µM or spermidine only at 300 µM. ROS levels were measured. This assay was repeated more than 3 times with similar results. (*B*) Potentiation of the flg22 ROS burst by spermidine is dependent on FLS2. Leaf disks from Col-0 or the *fls2* mutant were challenged with flg22 only at 20 nM or with spermidine at 300 µM. This experiment was performed twice with similar results. (*C*) Spermidine potentiates the elf18-induced ROS burst. Leaf disks were challenged with DW, elf18 at 50 nM, elf18 supplemented with spermidine at 400 µM, or with spermidine only at 400 µM. This experiment was performed twice. (*D*) Spermidine suppresses the flg22-induced calcium burst. Col-0_pMAQ2 leaf disks were treated with DW, flg22 at 25 nM, flg22 at 25 nM with spermidine at 400 µM, or with spermidine only. This experiment was repeated more than 3 times. Error bars represent standard errors.

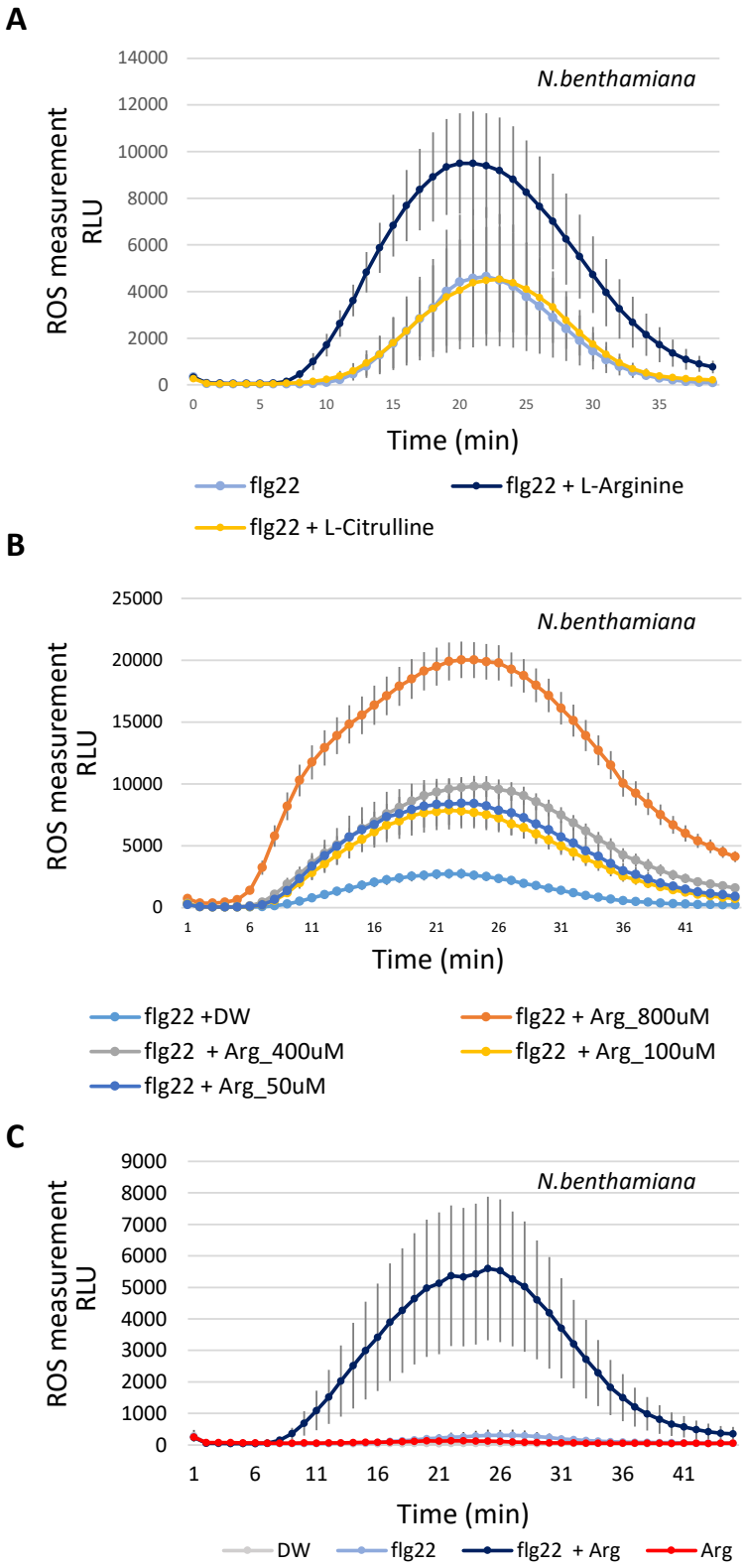

Figure S26. Arginine potentiates the flg22-induced ROS burst in *N. benthamiana*. *(A)* L-Arginine potentiates the flg22-induced ROS burst, but L-citrulline does not. flg22

was used at 10 nM, arginine and citrulline were used at 400 µM. This experiment was performed twice with similar results. *(B)* Dose-dependent effect of arginine on the flg22-induced ROS burst. flg22 was used at 100 nM and arginine at various concentrations. This experiment was performed twice with similar results. *(C)* The increase of the flg22-induced ROS burst by arginine is not due to an additive effect. flg22 was used at 10 nM and arginine at 400 µM. This experiment was repeated at least 3 times with similar results. Error bars represent standard errors.

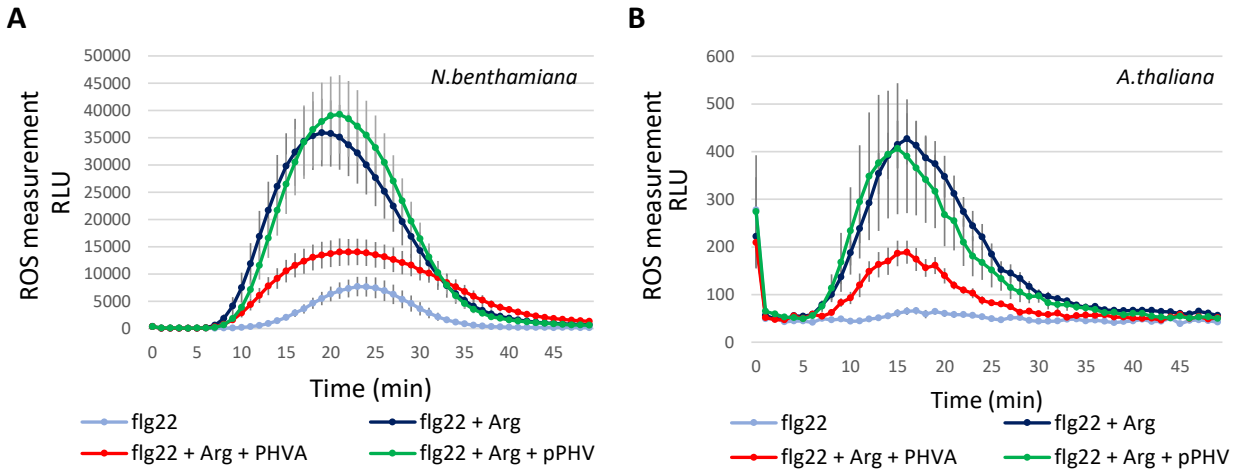

Figure S27. Phevamine A, but not prephevamine, suppresses the arginine potentiation of the flg22-induced ROS burst in both *N. benthamiana* and *A. thaliana*. *(A)* Phevamine A, but not prephevamine, suppresses the arginine ROS potentiation in *N. benthamiana.* flg22 was used at 5 nM; arginine, prephevamine and phevamine A at 300 µM. *(B)* Phevamine A, but not prephevamine, suppresses the arginine ROS potentiation in *A. thaliana.* flg22 was used at 5 nM; arginine, prephevamine, and phevamine A at 300 µM. PHVA: Phevamine A, pPHV: prephevamine. Experiments are representatives of 3 independent repeats with similar results.

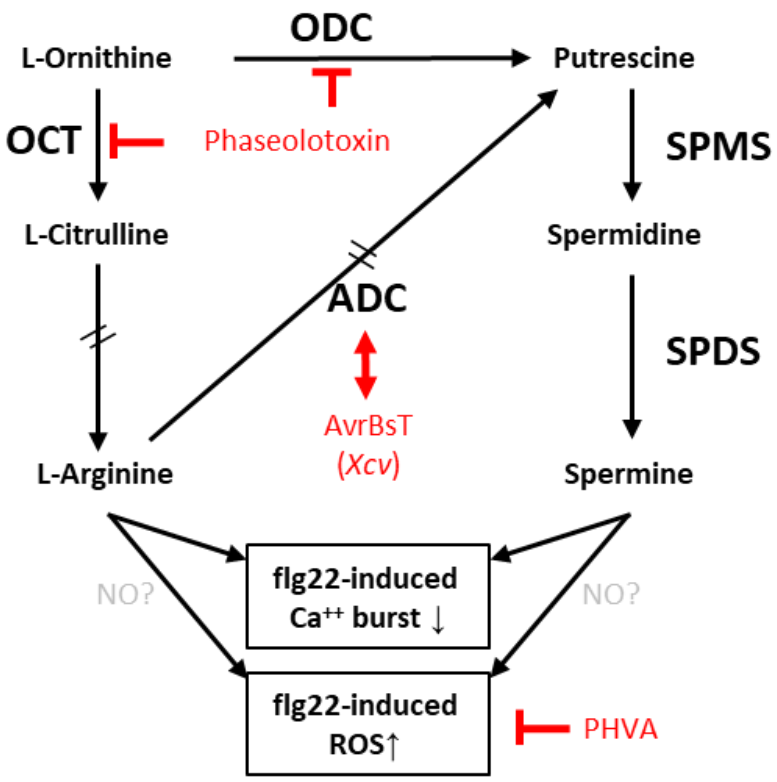

Figure S28. Arginine and polyamine biosynthetic pathways are targeted by pathogens via different mechanisms. Spermidine and L-arginine potentiate the flg22-induced ROS burst. The role of nitric oxide production in this potentiation remains uncertain (15). Phevamine A suppresses the spermidine/L-arginine potentiation of the flg22-induced ROS burst. Phaseolotoxin inhibits the synthesis of arginine and polyamines pathway by suppressing the activity of ODC and OCT, while phevamine A targets the potentiation mediated by spermidine and L-arginine. The effector AvrBsT from *Xanthomonas campestris* pv. *vesicatoria* (*Xcv*) interacts (red double arrow) with ADC1 in pepper (16). ODC: ornithine decarboxylase, OCT: ornithine carbamoyltransferase, ADC: arginine decarboxylase, SPDS: spermidine synthase, SPMS: spermine synthase, ROS: reactive oxygen species, NO: nitric oxide, PHVA: phevamine A. Double dashed arrows represent pathways with intermediates not shown. Reproduced from ref. (17) with permission from American Society for Microbiology.

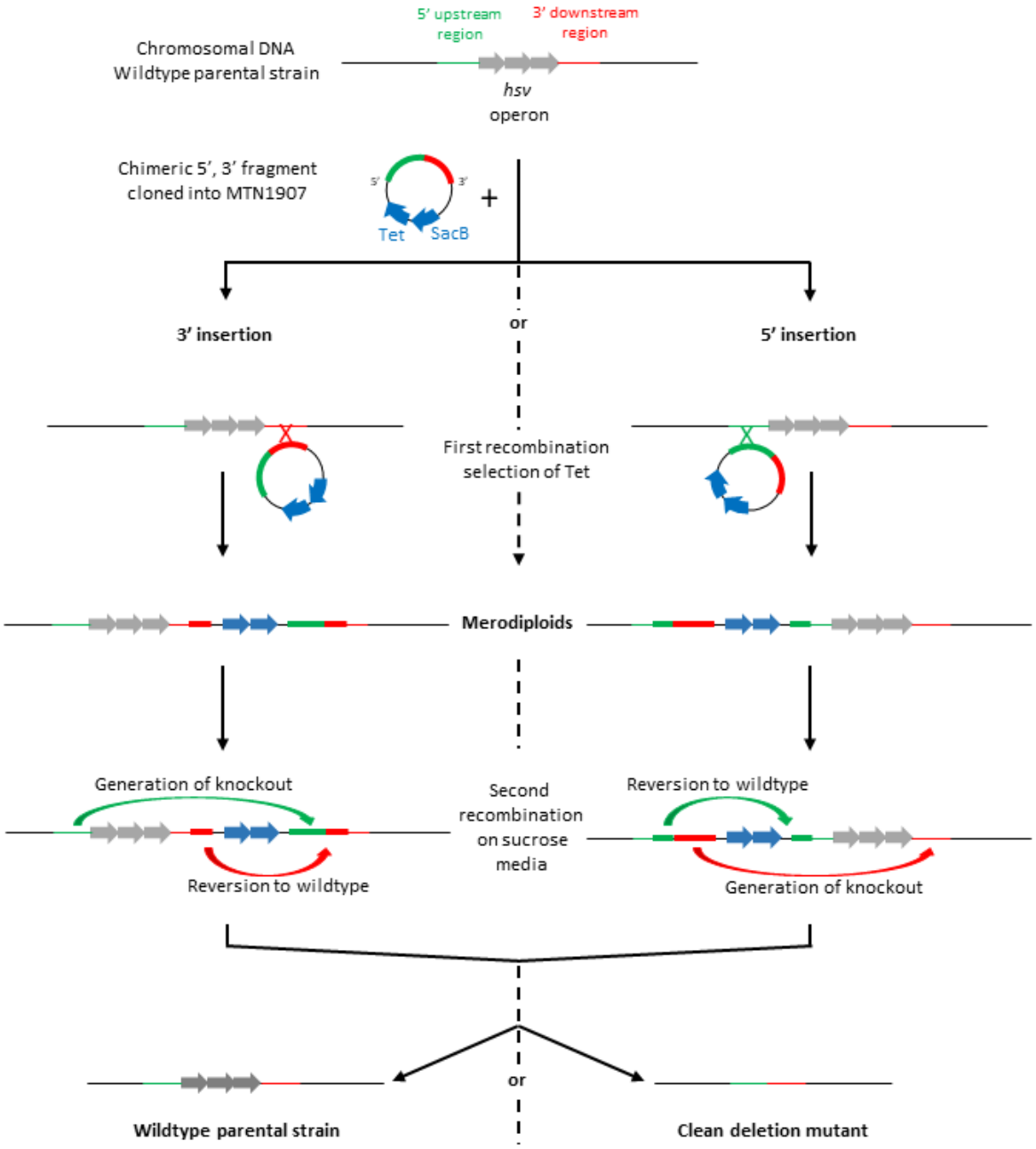

Figure S29. Strategy to generate *P. syringae* clean deletion mutants. A fusion of the 5' and 3' flanking region of the *hsv* operon was generated by chimeric PCR and cloned into MTN1907. After transformation of the parental strains (*Pto*, *Pto*-Cor $^{-}$, *Pto*D28E), the first recombination integrates the plasmid either at the 5 'or 3' end of the *hsv* operon. Merodiploids are selected on media containing tetracycline and genotyped by PCR. The second recombination event either leads to a reversion to the original locus or the generation of the clean mutant. Recombined strains were selected on plates containing sucrose (5%) and clean deletion mutants were identified by PCR (see Figure S30).

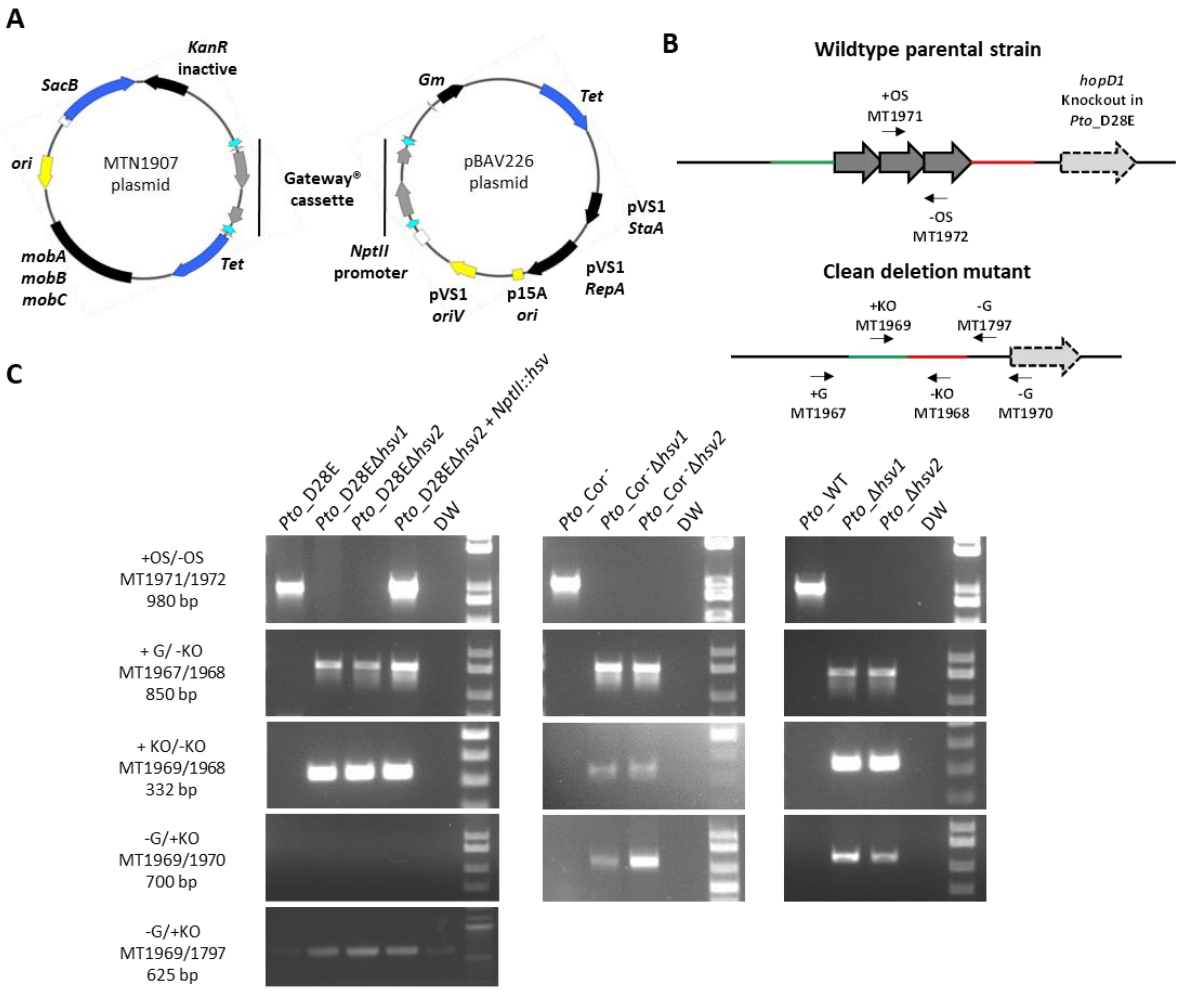

Figure S30. Genotyping of the clean deletion mutants and the complemented strain. *(A)* Graphical representation of the plasmids used for molecular manipulation of *P. syringae*. The left panel represents the MTN1907 plasmid used to engineer the mutants. The right panel represents the pBAV226 plasmid in which the *hsv* operon was cloned downstream of the *NptII* promoter for complementation of *Pto*D28E_Δ*hsv2*. Tet: confers resistance to tetracycline*; mobA, mobB, mobC*: RSF1010 mobilization genes; *ori*: high-copy-number origin of replication; *SacB*: a secreted levansucrase that renders bacteria sensitive to sucrose for counter-selection; *KanR*_inactive: aminoglycoside phosphotransferase gene inactive in *P. syringae*; pVS1 *StaA*: the stability protein from the *Pseudomonas* plasmid pVS1; pVS1 *RepA*: a replication protein; p15A *ori*: p15A origin of replication for propagation in *E. coli* cells; pVS1 *oriV*: origin of replication of the pVS1 plasmid; *Gm*: the gentamycin acetyltransferase. *(B)* Graphical representation of the *hsv* locus in the wildtype parental strains (*Pto*-WT, *Pto*-Cor ⁻, *Pto*D28E), and the clean deletion mutants. Arrows represent the primers used for the genotyping. OS: operon specific primer, G: genomic primer, KO: knockout primer, +: forward primer, -: reverse primer (see Supplementary Table S3 for primer sequences). (*C*) Analytical PCRs performed to confirm the genotype of the mutants generated in this study. PCR programs include a 1 min extension time, designed for amplification in mutant strains,

but too short for amplification in the wildtype parental strains with the exception of the PCRs using operon specific primers.

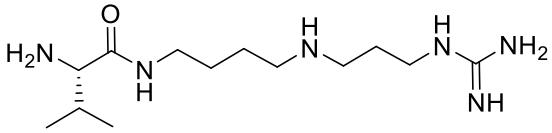

Prephevamine

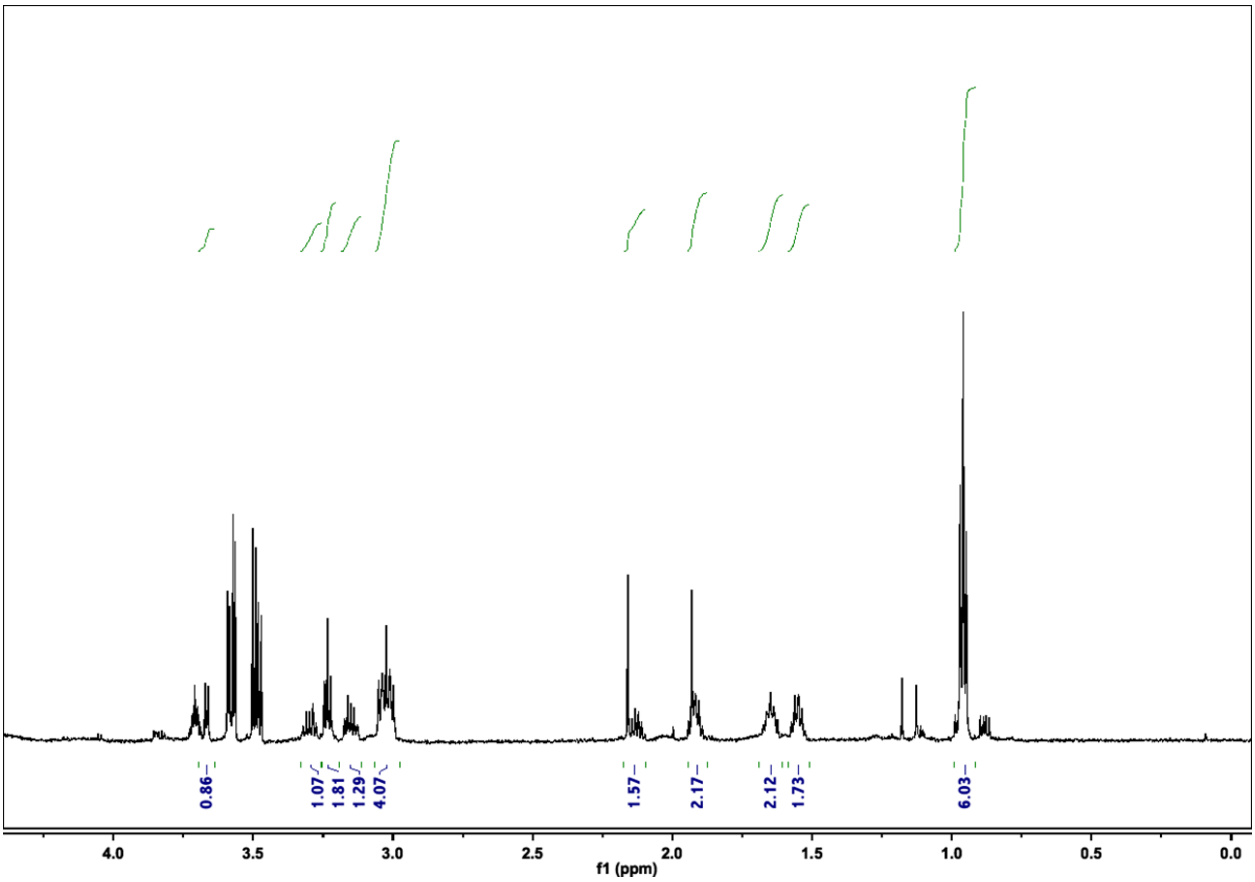

Figure S31. ^{1}H NMR (600 MHz) of *in vitro* purified prephevamine. Spectrum acquired in D_2O.

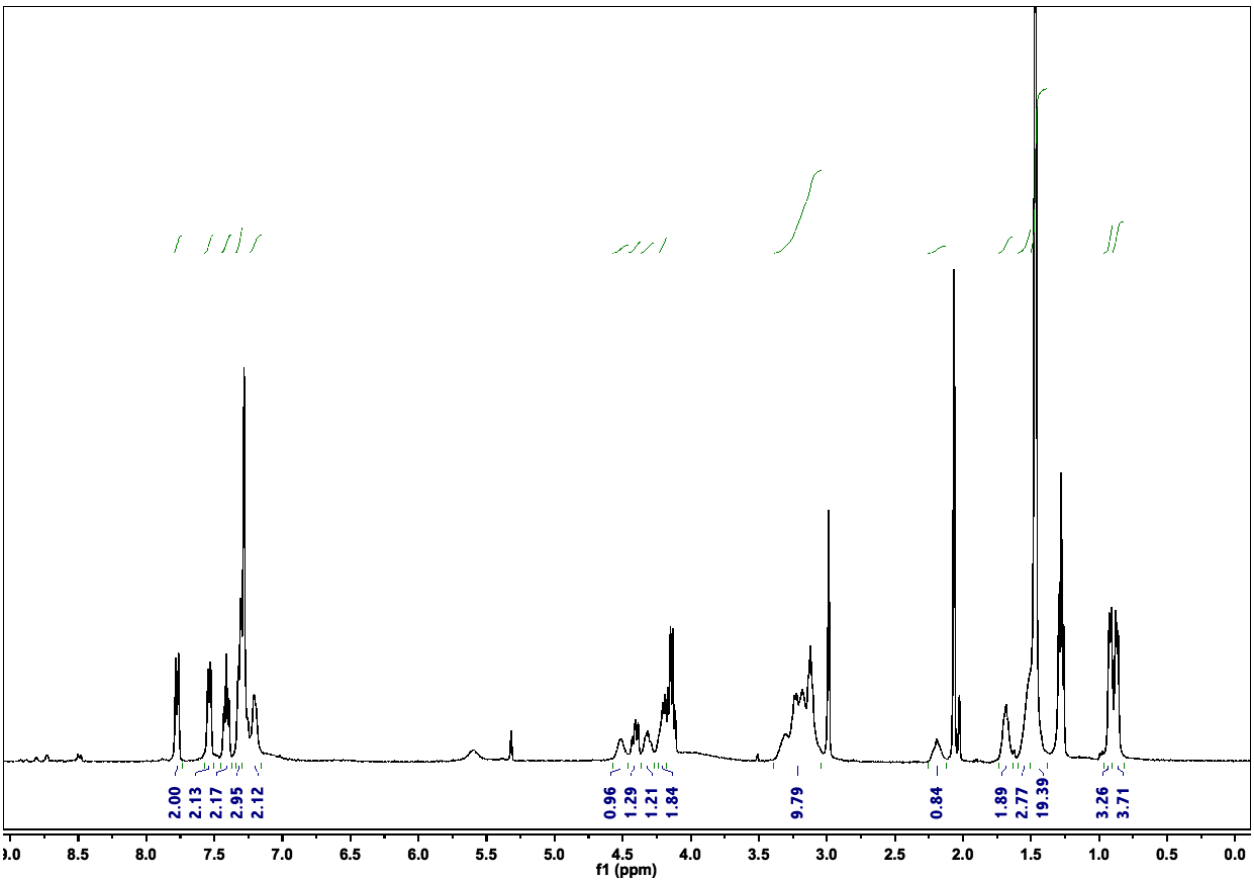

Figure S32. ^{1}H NMR (400 MHz) of Fmoc-(*S*)-Val-bis-Boc-spermidine (5). Spectrum acquired in $CDCl_3$.

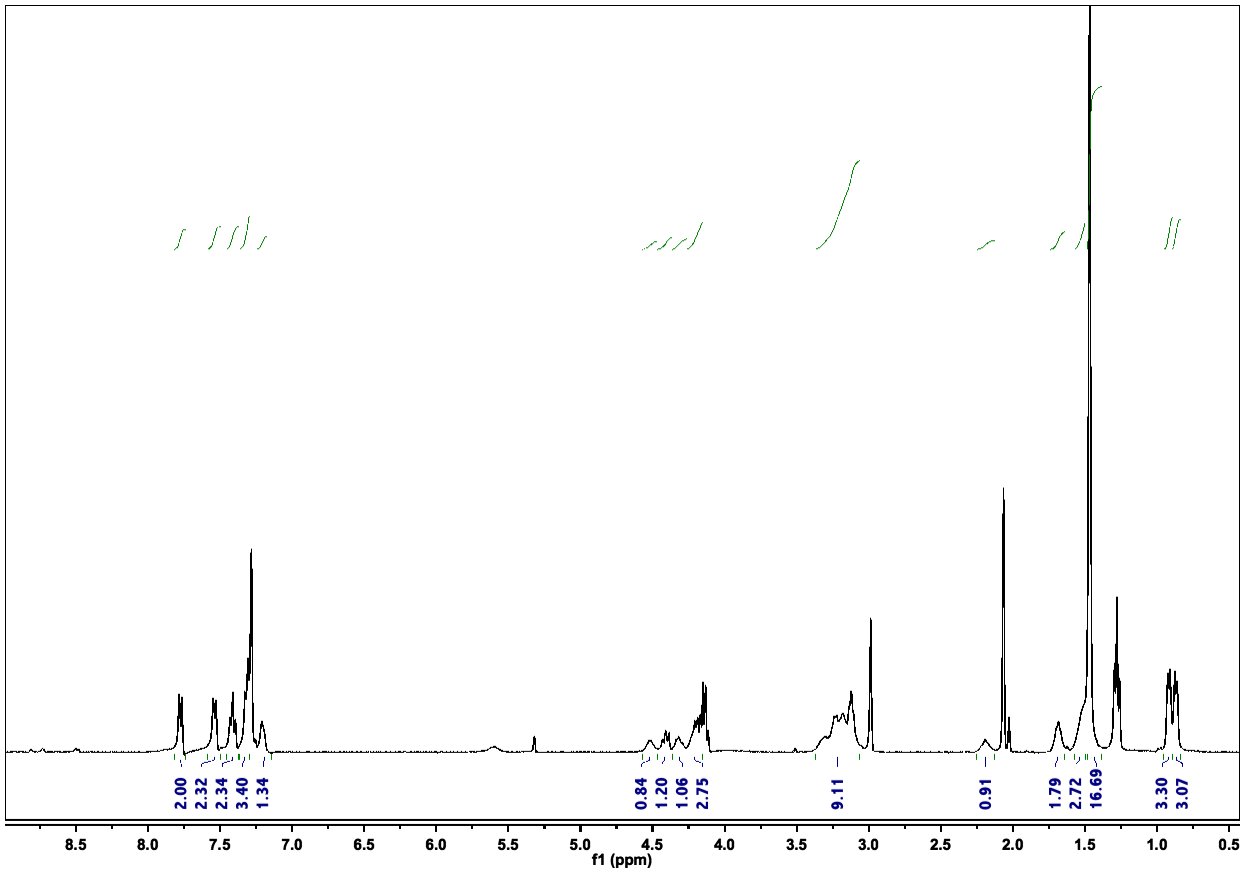

Figure S33. ^{1}H NMR (400 MHz) of Fmoc-(*S*)-Phe-(*S*)-Val-bis-Boc-spermidine (6). Spectrum acquired in $CDCl_3$.

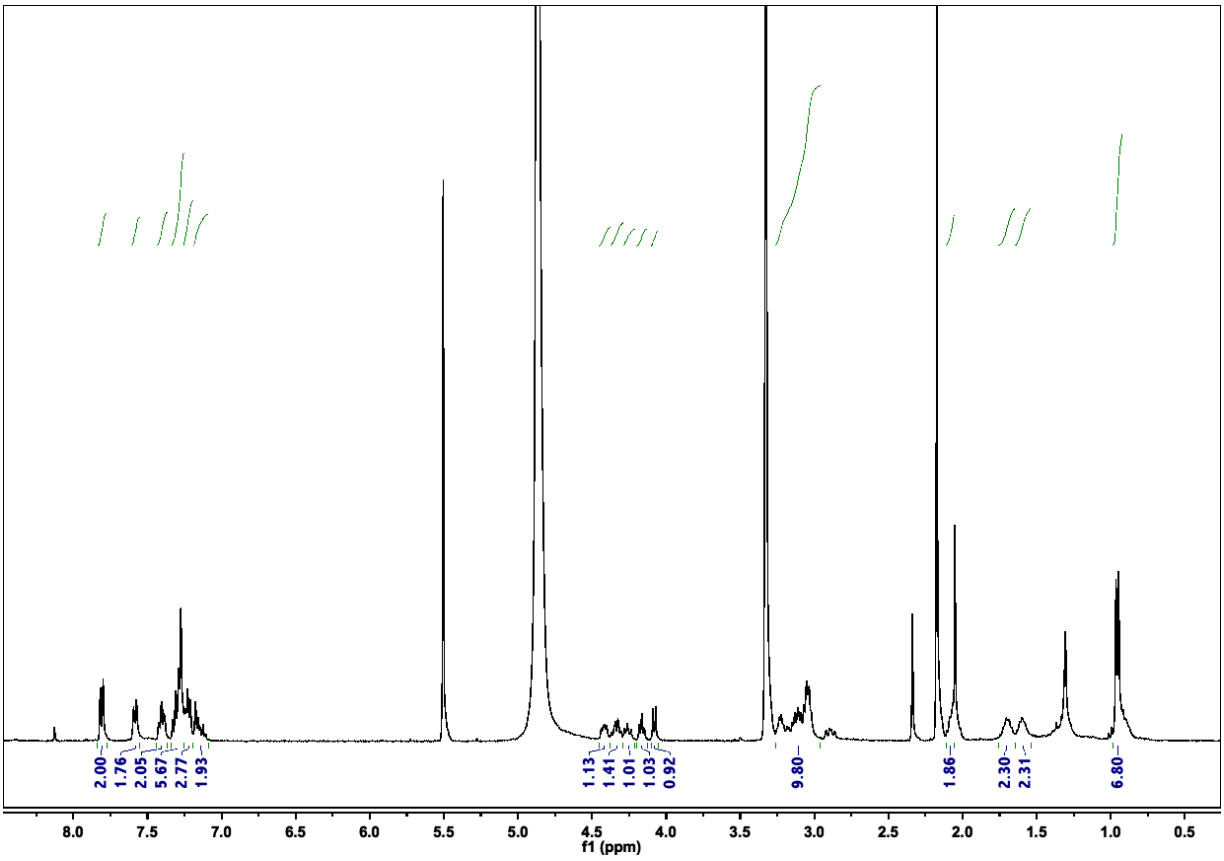

Figure S34. ^{1}H NMR (400 MHz) of Fmoc-(*S*)-Phe-(*S*)-Val-spermidine (7). Spectrum acquired in CD_3OD.

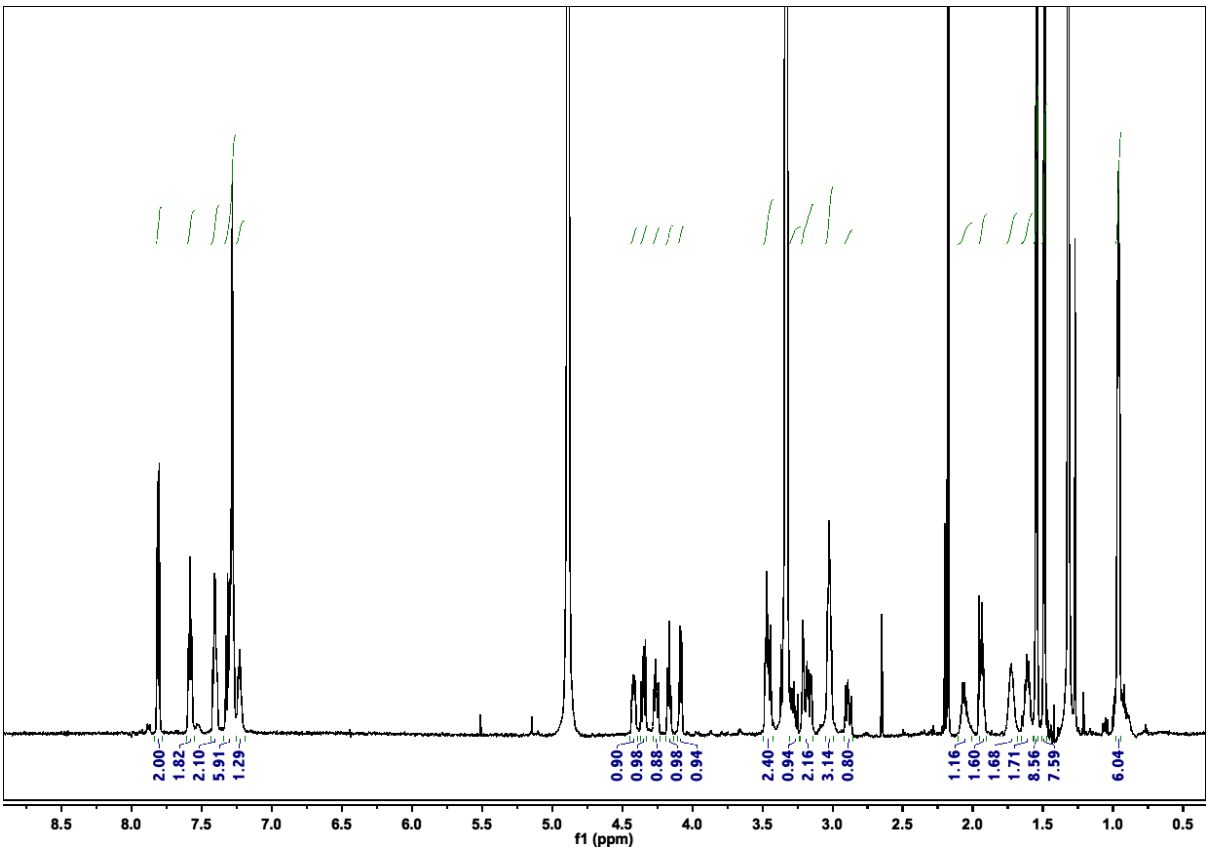

Figure S35. ^{1}H NMR (600 MHz) of Fmoc-(*S*)-Phe-(*S*)-Val-spermidine-*N,N*'-di-Boc-1*H*-guanidine (8). Spectrum acquired in CD_3OD.

References

1. Sambrook J & Russell D (2001) *Molecular Cloning: A Laboratory Manual* (Cold Spring Harbor, New York) 3rd Ed pp 6.4-6.12.
2. Mucyn TS*, et al.* (2014) Variable suites of non-effector genes are co-regulated in the type III secretion virulence regulon across the *Pseudomonas syringae* phylogeny. *PLoS Pathog* 10:e1003807.
3. Obranić S, Babić F, & Maravić-Vlahoviček G (2013) Improvement of pBBR1MCS plasmids, a very useful series of broad-host-range cloning vectors. *Plasmid* 70:263-267.
4. Choi K-H & Schweizer HP (2006) mini-Tn7 insertion in bacteria with single attTn7 sites: example *Pseudomonas aeruginosa*. *Nat Protoc* 1:153.
5. Marco ML, Legac J, & Lindow SE (2005) *Pseudomonas syringae* genes induced during colonization of leaf surfaces. *Environ Microbiol* 7:1379-1391.
6. Reyrat J-M, Pelicic V, Gicquel B, & Rappuoli R (1998) Counterselectable markers: untapped tools for bacterial genetics and pathogenesis. *Infect Immun* 66:4011-4017.
7. Knight H, Trewavas AJ, & Knight MR (1996) Cold calcium signaling in *Arabidopsis* involves two cellular pools and a change in calcium signature after acclimation. *Plant Cell* 8:489-503.
8. Kaur N*, et al.* (2008) Designing the polyamine pharmacophore: Influence of *N*-substituents on the transport behavior of polyamine conjugates. *J Med Chem* 51:2551-2560.
9. Wang J*, et al.* (2012) Synthesis, cytotoxicity, and cell death profile of polyaminoanthraquinones as antitumor agents. *Chem Biol Drug Des* 80:909-917.
10. Wang J*, et al.* (2014) Potent P-glycoprotein inhibition of emodin derivative: synthesis and biological evaluation. *Med Chem Res* 23:2106-2112.
11. Silby MW*, et al.* (2009) Genomic and genetic analyses of diversity and plant interactions of *Pseudomonas fluorescens*. *Genome Biol* 10:R51.
12. Thomas WJ, Thireault CA, Kimbrel JA, & Chang JH (2009) Recombineering and stable integration of the *Pseudomonas syringae* pv. *syringae* 61 hrp/hrc cluster into the genome of the soil bacterium *Pseudomonas fluorescens Pf*0-1. *Plant J* 60:919-928.
13. Ma S, Morris V, & Cuppels D (1991) Characterization of a DNA region required for production of the phytotoxin coronatine by *Pseudomonas syringae* pv. *tomato*. *Mol Plant Microbe Interact* 4:69-74.
14. Zeng W*, et al.* (2011) A genetic screen reveals *Arabidopsis* stomatal and/or apoplastic defenses against *Pseudomonas syringae* pv. *tomato* DC3000. *PLoS Pathog* 7:e1002291.
15. Yamasaki H & Cohen MF (2006) NO signal at the crossroads: polyamine-induced nitric oxide synthesis in plants? *Trends Plant Sci* 11:522-524.
16. Kim NH, Kim BS, & Hwang BK (2013) Pepper arginine decarboxylase is required for polyamine and γ-aminobutyric acid signaling in cell death and defense response. *Plant Physiol* 162:2067-2083.
17. Carrión VJ*, et al.* (2013) The *mangotoxin biosynthetic operon* (*mbo*) is specifically distributed within *Pseudomonas syringae* genomospecies 1 and was acquired only once during evolution. *Appl Environ Microb* 79:756-767.